



## Article

# Experimental and Numerical Heat Transfer Assessment and Optimization of an IMSI Based Individual Building Block System of the Kingdom of Bahrain

Payal Ashish Modi <sup>1,\*</sup> , Abdelgadir Mohamed Mahmoud <sup>1</sup> , Yousif Abdalla Abakr <sup>2</sup>  
and Abdulla Ebrahim Abdulqader <sup>3</sup>

<sup>1</sup> Razak Faculty of Tech and Informatics, University of Technology, Kuala Lumpur 54100, Malaysia; abdgadir.kl@utm.my

<sup>2</sup> Department of Mechanical Engineering, Nottingham University, Semenyih 43500, Malaysia; yousif.abakr@nottingham.edu.my

<sup>3</sup> Department of Mechanical Engineering, Bahrain Polytechnic, Isa Town P.O. Box 33349, Bahrain; ab.96@hotmail.com

\* Correspondence: payal.modi@polytechnic.bh

**Abstract:** The increase in energy consumption in Bahrain is a significant issue. Insulation blocks are crucial for reducing heat transfer from outside to inside buildings. However, there's limited research on the thermal performance of Bahrain's insulation building blocks. No research to date has been conducted in Bahrain to study the effect of plaster and insulation inserts on the R-value of the blocks. This study examines and optimizes the thermal resistance (R-value) of an 'Integrated Masonry System International, Ltd. (IMSI)' block, chosen due to its common use in Bahrain's commercial and residential construction. The study involves experimental analysis using a hot box setup and numerical analysis through the finite element method (FEM), along with assessing the impact of insulation inserts in the block's cavities. R-values are calculated and validated for accuracy. The R-value discrepancy between numerical and experimental findings is 2.411%, and between numerical and manufacturer's data is 5.743%. It is also observed that a 25 mm external plaster, as required by Bahrain's government (EWA), enhances the R-value by 79.34%. Furthermore, optimizing the IMSI block's height increased the R-value by 10.67%.

**Keywords:** building block system; insulation blocks; energy consumption; thermal resistance; thermal insulation; R-value; cavity; IMSI individual block



**Citation:** Modi, P.A.; Mahmoud, A.M.; Abakr, Y.A.; Abdulqader, A.E. Experimental and Numerical Heat Transfer Assessment and Optimization of an IMSI Based Individual Building Block System of the Kingdom of Bahrain. *Buildings* **2024**, *14*, 2012. <https://doi.org/10.3390/buildings14072012>

Academic Editors: Yu Huang, Siwei Lou and Yukai Zou

Received: 10 June 2024

Revised: 22 June 2024

Accepted: 27 June 2024

Published: 2 July 2024



**Copyright:** © 2024 by the authors. Licensee MDPI, Basel, Switzerland. This article is an open access article distributed under the terms and conditions of the Creative Commons Attribution (CC BY) license (<https://creativecommons.org/licenses/by/4.0/>).

## 1. Introduction

In the modern world, the changes in the global climate and the high rate of fossil fuel consumption have affected all the economic sectors, keeping the building sector as the third largest after industry and agriculture [1]. Globally, around 40% of the energy demand is consumed by buildings, mostly for heating and cooling purposes, which further account for one-third of greenhouse gas emissions [2]. Moreover, the opaque envelopes (mainly the walls) of a building are responsible for 10–45% of total energy losses [3]. Cool roofs, which reflect more sunlight, were found to lower the temperature of the walls they adjoin, enhancing the walls' thermal performance by up to 30% [4]. Filling of argon gas as insulation within the windowpanes play an important role in thermal performance of windows. One of the test results indicated that the thermal performance decreased by 10.9% when the argon gas filling rate was reduced from 95% to 0%. In same study the simulation results showed that the thermal performance of windows that were insulated using only glazing decreased by 22.6% with the decrease in the argon gas filling rate; the thermal performance of the double-glazed windows also decreased by 13.6% [5]. The in-situ test results showed that winter performance for triple glazed Low-E glass was better

than double glazed [6]. Another analysis points to the importance of the roof, as it is the major contributor to the thermal load, followed closely by columns and slabs, with 44.2% of the overall cooling load [7]. Therefore, the design of each building element is crucial in energy efficiency initiatives, including the building blocks used to construct the wall systems. In general, the life of a building is 40–50 years or more, and if appropriate measures are taken to construct the wall systems, then by 2050, the building energy demand globally can be reduced by one-third [8]. The Kingdom of Bahrain is a Gulf country that experiences a hot and humid climate for most of the months of the year. In the last twenty years in Bahrain, the total primary energy supply increased by 4.2%, total final energy consumption increased by 5.3%, and non-industrial electricity consumption increased by 6.6% per year [9]. According to the MEW-Ministry of Electricity and Water [10], there has been an increment of 5% in the average growth rate of the population during the period of 2014 to 2018. The primary energy consumption for Bahrain increased from  $1.11 \times 10^8$  MWh in 2000 to  $1.96 \times 10^8$  MWh in 2019, growing at an average annual rate of 3.14% [11]. Per capita energy consumption reached 112.81 MWh in 2019 (three times the Middle East average and five times the global average), whereas electricity consumption per capita was 21 MWh, which was five times the Middle East average and 7 seven times the global average [12]. The residential sector used most of the grid electricity, at 49.5% of total grid consumption, during the baseline period, followed by the commercial sector, accounting for 36.6% during the same period. Approximately 60% of the residential sector's annual electricity is used for air conditioning, which is similar to the commercial sector, at 55% [9]. Therefore, the walls of the residential and commercial sectors have a high potential for significant energy efficiency improvements.

The performance of blocks mainly depends on three parameters—insulation materials used in the block, design of cavities of the block, and aggregate materials used to build the block. Various approaches have been presented to investigate the effect of insulation materials experimentally and numerically [13–16]. In [13], when phase change materials (PCM) were used in building blocks, significant improvements in thermal regulation, reducing indoor temperature fluctuations, were observed. The latent heat storage capacity of PCMs helped absorb excess heat during the day and released it at night, leading to a more stable indoor environment. In a computational study in the USA, PCM-integrated walls lead to significant energy savings. The simulations indicated up to 20% reduction in annual heating and cooling energy consumption [14]. In [15], using experimental and computational study, it was found that Polyisocyanurate (PIR) insulation provides excellent thermal resistance. The research in [16] focused on the advanced fabrication and characterization of aluminum hydroxide aerogels produced from aluminum waste. Aluminum hydroxide aerogels exhibit low thermal conductivity, making them effective thermal insulation materials. Further, studies like [17–19] demonstrate as to how certain cavity designs and certain combinations of insulation and cavity design can remarkably improve the thermal performance of building blocks. Additionally, some materials, if used as aggregates, like geopolymers [20], date palm ash [21], red mud [22], and sustainable materials reducing carbon footprints [23], also play a huge role in improving the thermal performance of blocks.

Thermal testing of building blocks is mainly conducted using two methods- the experimental method and the numerical method. Under the experimental method, Martinez, L., in 2018, explored the use of infrared thermography for the measurement of thermal performance of building blocks. The study very well demonstrated the use of infrared cameras to find thermal bridges, defects, or areas of heat loss in a building system [24]. Saad Alqahatani's study aimed to develop, produce, and calibrate a hot box calorimeter at a reasonable price for thermal testing of the components of building envelope. This hot box can conduct a conventional thermal experiment, which involves monitoring heat flux, surface temperatures, and air temperatures however, carrying an advantage of small size and simpler thermal testing methods [25]. Another experimental study by Patel, S. in 2020 focused on the evaluation of the R-value of sustainable building materials like recycled

concrete and natural fiber composites using the heat flow meter method [26]. Numerical studies have turned out to be equally important as they account for predicting the thermal performance of different geometric variations and material properties. Numerical studies on the thermal behavior of PCM-integrated concrete blocks use computational fluid dynamics (CFD) and FEA to model the thermal behavior of concrete blocks integrated with phase change materials (PCMs). The simulations conclude that PCM integrated walls increases the thermal comfort of the buildings [27]. It is evident that the geometry of blocks, joints of the blocks and thermophysical properties of building materials significantly affect the thermal behavior of the entire wall systems. This investigation is done in detail in [28] using numerical analysis by adopting well known CFD program. Results of another study that employs numerical simulations to evaluate the thermal resistance of blocks with different concrete solid mixture, the cavities infill material, and the geometry configuration of the [29].

### 1.1. Motivation

The investigation of the thermal resistance of blocks used to build the walls is of high importance as a major part of the building walls are made up of concrete blocks. The comparative study done for experimental and theoretical results depicts the importance of using the hot-box setup. It proved that the development of an experimental unit to measure the thermal efficiency of walls can be helpful to provide real-time results that can later contribute to propose more effective insulation techniques [30]. Moreover, as the Kingdom of Bahrain is a Gulf country, the thermal efficiency of walls is of high importance. This present paper attempts to investigate, experimentally and numerically, the thermal performance of a widely used block for the construction of buildings in Bahrain, named the IMSI block. IMSI stands for 'Insulated Reinforced Masonry System International, Ltd'. This block is a concrete block with polystyrene insulation inserts with a unique design and structural integrity not found in other insulated masonry assemblies. The test results thus obtained will further be extended and used in future research work to optimize the design of the block for improved thermal resistance, thereby reducing energy consumption and hence benefiting the overall country.

### 1.2. Scope

Few approaches were already developed in similar areas [31–33]. This paper is an extension and improvement of the mini hot box developed by P. Modi in 2016 [32]. The latest design of the insulation block widely used in Bahrain, the IMSI block, is tested to evaluate the thermal resistance values using the hot box experimental setup. A series of measurements are taken to achieve a steady state condition and to reduce the effect of the outdoor environment while ensuring that the outdoor/indoor conditions are well simulated within the box to maintain the accuracy of measurements as far as possible. Moreover, a numerical approach of the same IMSI concrete block is investigated, wherein the block design is created using SolidWorks software (2021-2022) and simulated using Ansys software R-15.0 (2021-2022) at a steady-state thermal condition. The experimental, numerical, and manufacturer's thermal resistance  $R$  values, thus obtained, are well compared and validated. Moreover, the construction companies need to follow an appropriate set of rules set by the Bahrain government [33] for building of walls in which for IMSI blocks, two layers of plaster of 25 mm each on inner and outer sides of the walls are to be provided. The laboratory does not conduct tests for blocks with plaster and no research to date has been conducted in Bahrain to study the effect of plaster on the  $R$ -value of the blocks. So, neither the construction companies nor the manufacturing companies have any idea about the improvement in the  $R$ -value. Therefore, in the present research, the experimental and numerical tests are performed for blocks with plaster and the improvement in the  $R$ -value is clearly presented.

## 2. Methodology

### 2.1. Thermal Insulation

Thermal insulation is a term used for a material or a product that can reduce the rate of heat transfer. The usage of insulation material in the building blocks is important as it helps to retard the energy loss through the wall system thereby reducing the electricity consumption and hence the monthly electric bill while maintaining the comfortable indoor thermal environment.

### 2.2. Thermal Resistance (R-Value)

If a block of an external wall of a building is considered as shown in the Figure 1, then the modes of heat transfer developed through the block surface include combination of conduction, convection, and radiation, for the heat to flow from hot to the cold side (left to right side). Neglecting the effect of radiation, the convection heat transfer takes place on either side of the block which includes a hot air and hot block surface on the right side while a cold surface and cold air on the left side of the block which can be applied as

$$q_{h,convection} = q_{conduction} = q_{c,convection} \quad (1)$$

where  $q_{h,convection}$  is the convection heat transfer rate per unit area ( $W/m^2$ ) from the heat source to the hot surface of the block,  $q_{conduction}$  is the conduction heat transfer rate per unit area ( $W/m^2$ ) through the solid block and  $q_{c,convection}$  is the convection heat transfer rate per unit area ( $W/m^2$ ) from the cold surface of the block to the cold air. It can be written in terms of temperatures of Figure 1 as shown in Equation (2):

$$\frac{T_{\infty 1} - T_h}{R_{hot\ air}} = \frac{T_h - T_c}{R_{block,exp.}} = \frac{T_c - T_{\infty 2}}{R_{cold\ air}} \quad (2)$$

where  $T_{\infty 1}$  ( $^{\circ}C$ ) is the temperature of the hot air developed by the heat source;  $T_h$  ( $^{\circ}C$ ) is the hot surface temperature of the block facing the heat source and hot air;  $T_c$  ( $^{\circ}C$ ) is the cold surface temperature of the block; and  $T_{\infty 2}$  ( $^{\circ}C$ ) is the cold air temperature. While,  $R_{hot-air}$  ( $m^2 \cdot ^{\circ}C/W$ ) and  $R_{block-exp}$  ( $m^2 \cdot ^{\circ}C/W$ ) is the thermal resistance of hot air and  $R_{cold-air}$  ( $m^2 \cdot ^{\circ}C/W$ ) is the thermal resistance of cold air for the block. The thermal resistances of each layer are defined as in Equation (3):

$$R_{hot\ air} = \frac{1}{h_h}, R_{cold\ air} = \frac{1}{h_c}, R_{block} = \frac{l}{k} \quad (3)$$

where  $h_h$  ( $W/m^2 \cdot ^{\circ}C$ ) and  $h_c$  ( $W/m^2 \cdot ^{\circ}C$ ) are the convective heat transfer coefficients for hot and cold air;  $l$  (m) is the width of the block; and  $k$  ( $W/m \cdot ^{\circ}C$ ) ( $W/m^{\circ}C$ ) is the thermal conductivity of the block

$$R_{block,num.} = \frac{T_h - T_c}{q} \quad (4)$$

where  $R_{block,num.}$  ( $m^2 \cdot ^{\circ}C/W$ ) is the value of thermal resistance obtained through Ansys simulation,  $T_h$  ( $^{\circ}C$ )  $T_h$  and  $T_c$  ( $^{\circ}C$ ) are, respectively, the values of temperatures for the hot and cold surfaces of the block, while  $q$  ( $W/m^2$ ) is the value of the heat flux.

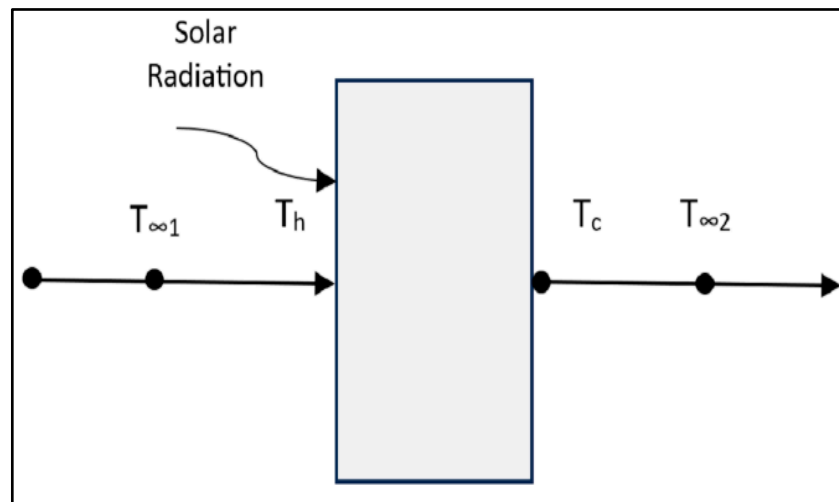


Figure 1. Thermal resistance network.

### 2.3. Heat Transfer Coefficient of Air

To calculate the  $R_{\text{block,exp.}}$  ( $\text{m}^2 \cdot ^\circ\text{C}/\text{W}$ ), it is necessary to calculate the amount of heat flowing through the block. Therefore, it is required to identify the properties of air at the average temperature on the hot side of the block (Figure 1). The properties are density, dynamic and kinematic viscosity, specific heat, thermal conductivity, thermal diffusivity, and coefficient of thermal expansion of air. The convective heat transfer coefficient 'h' can be calculated by Equation (5):

$$h = \frac{\text{Nu} * k}{x} \quad (5)$$

where Nu (dimensionless) is the Nusselt number,  $k$  ( $\text{W}/\text{m} \cdot ^\circ\text{C}$ ) is the thermal conductivity of air,  $x$  (m) is the length of the heat source, which in this case is the vertical flat copper plate. The Nu number can be obtained using Equation (6):

$$\text{Nu} = \left\{ 1 + \left[ \frac{0.493 * \text{Ra}^{0.293}}{1 + (6310/\text{Ra})^{1.36}} \right] \right\}^{1/3} \quad (6)$$

where Ra (dimensionless) is the Rayleigh number, Gr (dimensionless) is the Grashoff number and Pr (dimensionless) is the Prandtl number which can be obtained by using Equations (7)–(9) respectively:

$$\text{Ra} = \text{Gr} * \text{Pr} \quad (7)$$

$$\text{Gr} = \frac{g\beta(T_1 - T_2)x^3}{\nu^2} \quad (8)$$

$$\text{Pr} = \frac{\mu C_p}{k} \quad (9)$$

where  $g$  ( $\text{m}/\text{s}^2$ ) is the gravitational acceleration,  $\beta$  ( $\text{K}^{-1}$ ) is the coefficient of volume expansion of air,  $x$  (m) is the length of the heat source,  $\nu$  ( $\text{m}^2/\text{s}$ ) is the kinematic viscosity of air, and  $T_1$  ( $^\circ\text{C}$ ) and  $T_2$  ( $^\circ\text{C}$ ) are, respectively, the temperatures of the heat source and hot air. The properties of air are obtained from standard resources at the average temperature of  $T_1$  and  $T_2$  [34,35].

### 2.4. Concrete Insulation Blocks in Bahrain

Due to the geographical location of Bahrain, it experiences a hot climate for most of the months of the year, i.e., from April to November. The average temperatures in Bahrain from the years 2015 to 2024 [36] are presented in Figure 2. The average annual maximum temperature is  $41$   $^\circ\text{C}$  in the month of July, and the average annual minimum temperature

is 21 °C in the months of January and February. Also, to note that the average annual relative humidity in the past 10 years ranges between 53% and 63% [37]. Because of this reason, the effective heat felt is much higher than the actual temperature. These reasons contribute to the fact that residents rely heavily on air-conditioners to obtain comfortable indoor temperatures. It was estimated that 6.34 TWh of electrical energy was used for cooling during May to October 2016, most of which was utilized during the June–September months, and these results were translated into a total electricity cost of 507.443 million USD [38].

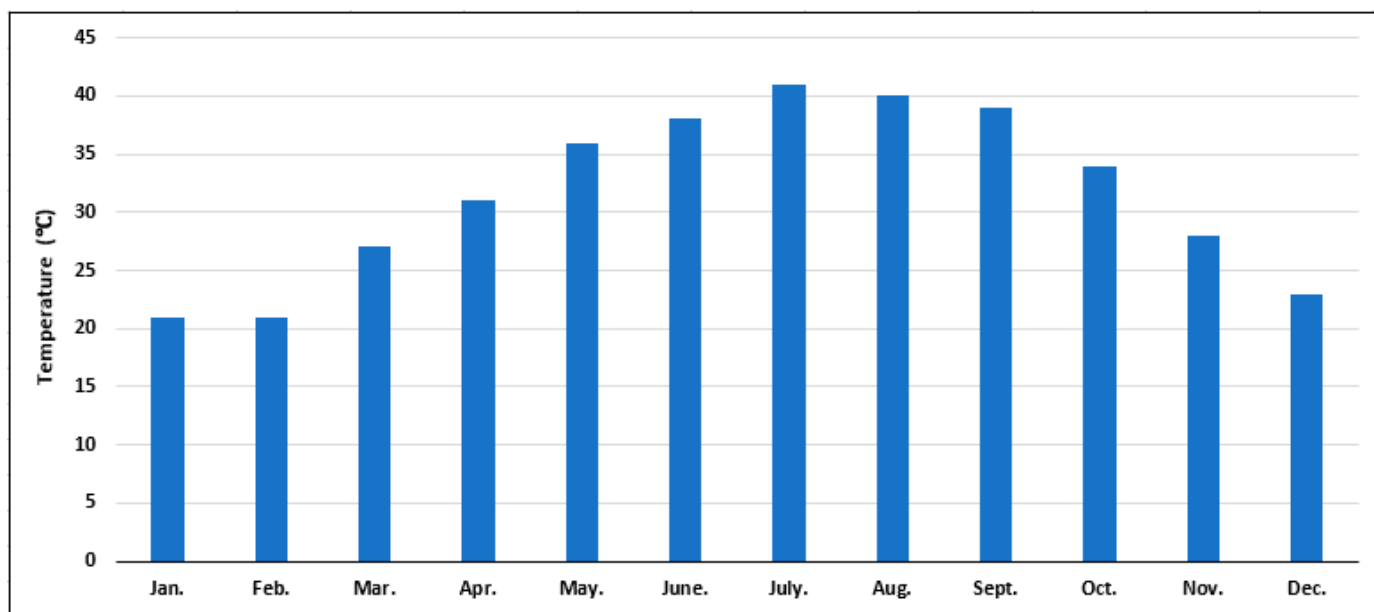


**Figure 2.** Monthly average temperatures in Bahrain from 2015 to 2024.

There are two major energy efficiency opportunities in Bahrain; first to significantly reduce the electricity used in buildings, and second, to improve the thermal efficiency of buildings. In the present work, the second approach is discussed that includes the building blocks of Bahrain. Better thermal insulation on the external walls of buildings can help reduce the heat transfer from outdoors to indoors in summer and from indoors to outdoor in winter. Varieties of blocks are manufactured in Bahrain, as shown in Figure 3a,b below. The simple blocks (Figure 3a) are used to build compound walls of a house or for the partition walls between two rooms of a house or for the pavement. However, there are some other blocks that are specifically manufactured to build the outer walls of a house or a building, as shown in Figure 3b. These blocks are called ‘Insulation blocks’. These blocks have insulation inserts within the cavities of the blocks. The slotted blocks were commonly preferred up to 2018. However, in the present day, IMSI and Sandwich are preferred by both the construction companies and the house owners. In accordance with the discussion with the manufacturing companies, it was clear that after a few years, the Sandwich blocks had an issue with the formation of cracks on the walls, while no such issues were observed in the IMSI blocks. Eventually, considering that the IMSI blocks are the most reliable blocks in today’s time and are widely used in the construction of buildings in Bahrain, an IMSI block from the ‘Bahrain Blocks’ company was selected in the present work for further investigation.



**Figure 3.** Blocks manufactured in Bahrain, (a) Simple blocks (b) Insulation blocks.

### 2.5. Experimental Method

The experimental hot box unit was initially developed and tested by P. Modi in 2016 [32]. The present experimental work is an extension of this previous work. While keeping the same internal dimensions of the hot box (Figure 4) [32], certain modifications (Figure 5) in the design of the hot box were carried out to reduce the heat losses and increase the efficiency of the measurements.

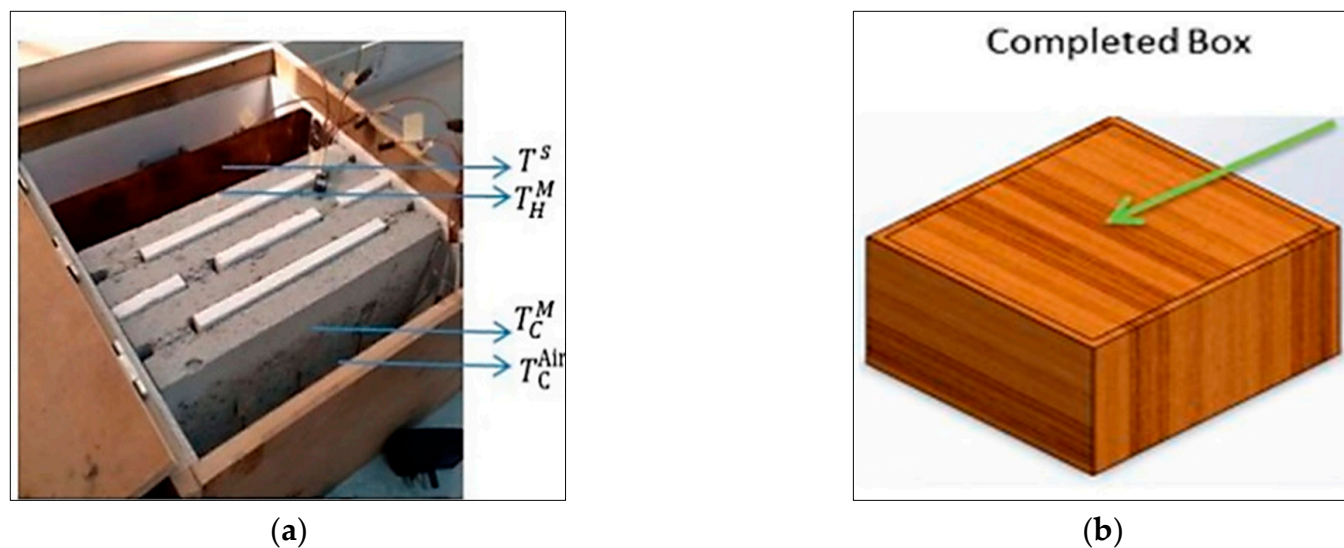
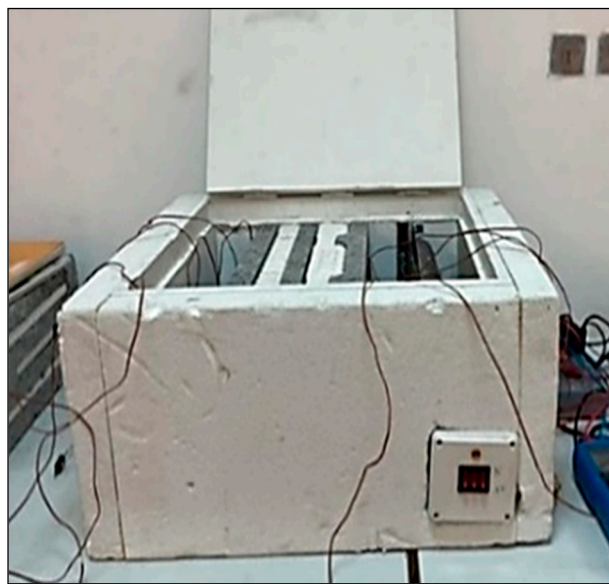


**Figure 4.** The previous setup of the hot-box experiment. (a) The outer surface of the hot box was not insulated [32]. (b) The top surface of the hot box was not insulated [32].



(a)



(b)



(c)



(d)

**Figure 5.** Improvements in the hotbox setup for present work. (a) The outer surface of the hot box is insulated using polystyrene to reduce the heat losses. (b) A Pico Log TC-08 data logger, with specifications [39] was used for temperature measurement and recording. (c) The top surface of the hot box is well sealed with aluminum tape. A heat leak detector is used to check the heat losses. Red light shows that leakage of heat exists. (d) The hot box is further sealed from the top and sides with aluminum foil up-to the point when green light appeared.

For current work, Figure 6 shows the dimensions of the hot-box experimental setup, while the internal view of the hot box and the three conditions of the IMSI block under consideration are presented in Figure 7.



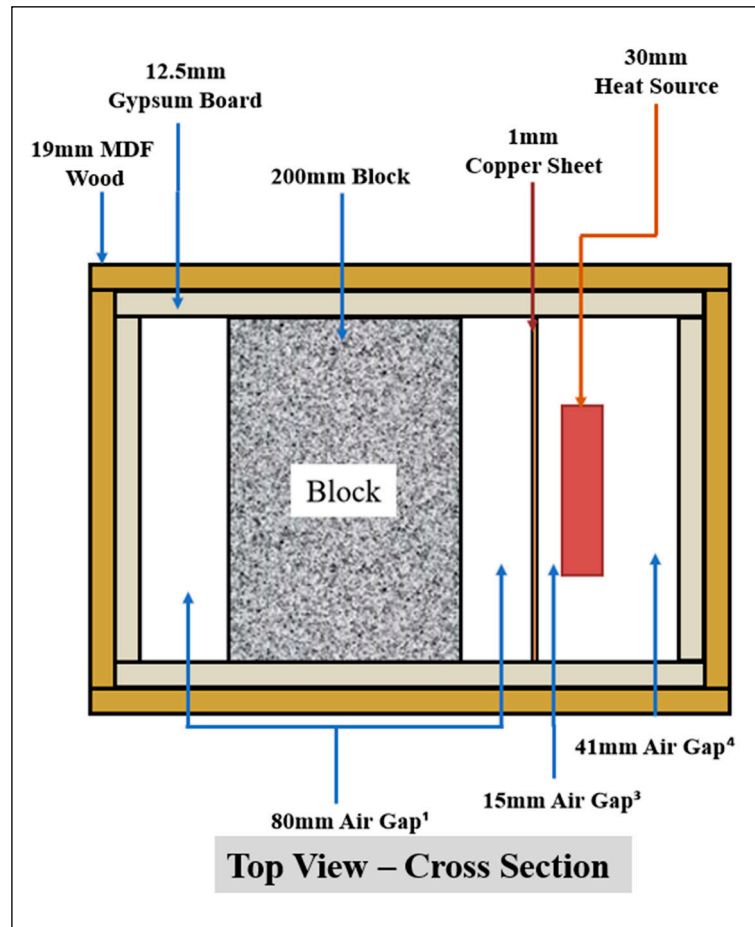


Figure 6. A diagram showing the dimensions of the experimental setup.

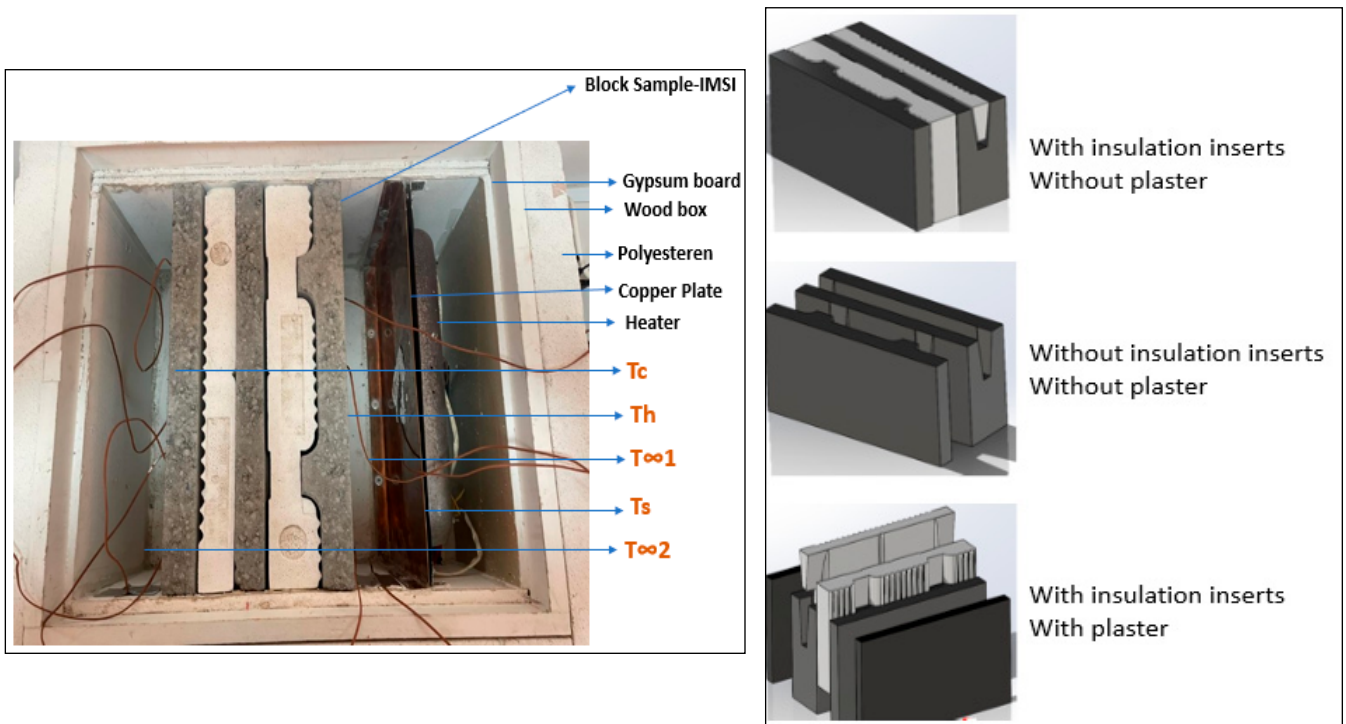
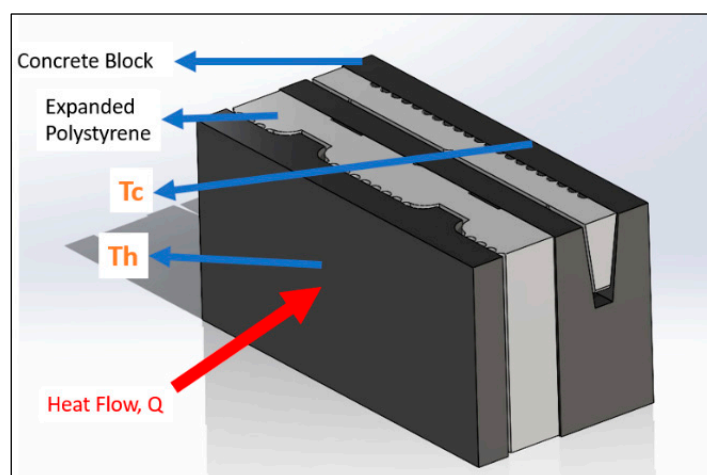


Figure 7. Final experimental setup and the three conditions of the IMSI block under consideration.

The widely used IMSI insulation block of Bahrain was selected for testing purposes. The block was placed in the box such that two air gaps existed before and after the block. One side of the block has a heater that is connected to an electric supply through a variac that maintains the power supply. A copper plate ( $T_s$ ) is attached to the heater to ensure the appropriate distribution of heat through the box. The heat is transferred from the copper plate to the hot side of the block ( $T_s$ ) through an air gap ( $T_{\infty 1}$ ). The heat then flows through the blocks' cold side ( $T_c$ ) into the air gap on the other side of the box ( $T_{\infty 2}$ ). Thermocouples are connected to each of these layers to measure their respective temperatures, and a Pico Log TC-08 data logger, from Pico Technology Ltd., (Wales, UK) is used to extract the measurements every 15 min and noted in an Excel sheet.

## 2.6. Numerical Method

The thermal resistance of the IMSI block in the experimental setup was investigated by conducting a numerical analysis using Ansys simulation software R15.0 (2021-22). The design of the block was prepared using the design software SolidWorks (2021-22), as shown in Figures 8 and 9. Detailed designs are available in Appendix A Figures A1–A3. Figure 8 is the setup for the numerical investigation of the IMSI block, wherein the input values correspond to the ones from the experimental method to furthermore check for its validity. Three different variables are considered, which include the hot temperature ( $T_h$ ) in  $^{\circ}\text{C}$ , cold temperature ( $T_c$ ) in  $^{\circ}\text{C}$ , and heat flux ( $Q$ ) from the direction of the heat flow in  $\text{W}/\text{m}^2$ .

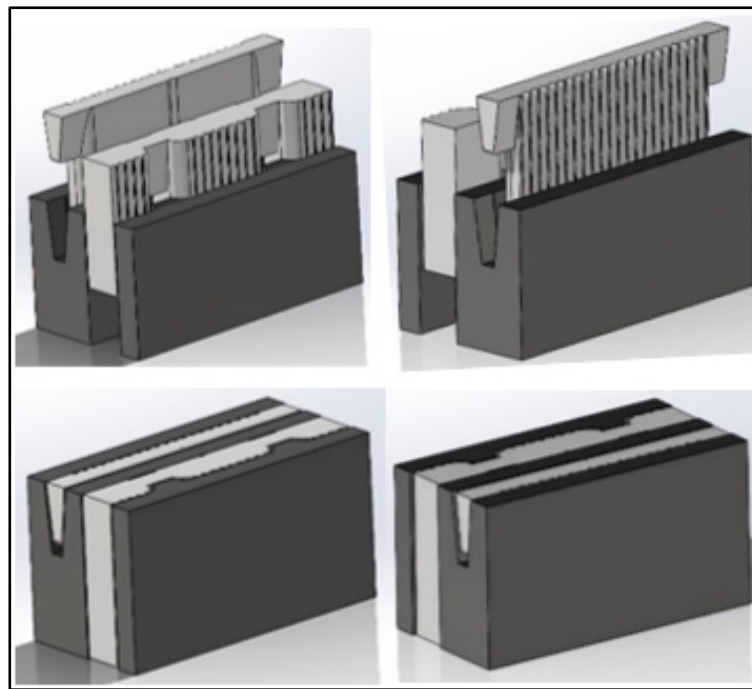


**Figure 8.** 3D Design of the Numerical Setup.

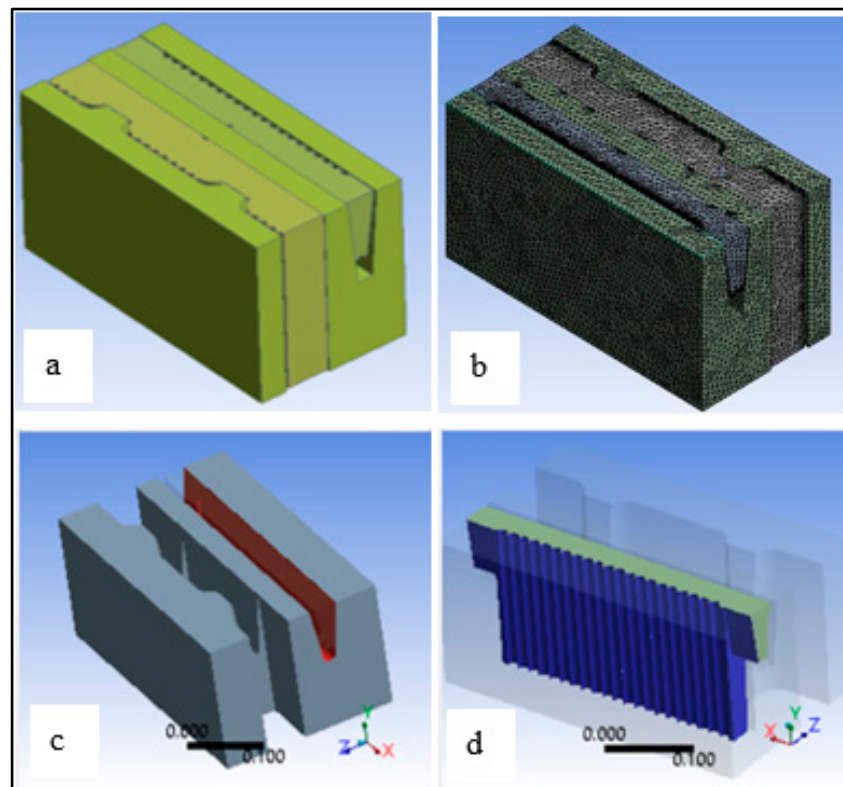
Moreover, the IMSI block assembly is made from concrete material with a thermal conductivity of  $2.25 \text{ W}/\text{m K}$  [40] while the insulation inserts are made of expanded polystyrene with a thermal conductivity of  $0.034 \text{ W}/\text{m K}$  [41]. Moreover, to analyze the effect of plaster on the performance of the block, it is worth noting that the plaster was considered with a thermal conductivity value of  $0.08 \text{ W}/\text{m K}$  [33].

Figure 9 shows the SolidWorks assembly of the IMSI block where the front and back isometric view is shown alongside its exploded view to further illustrate the components of the assembly. For the dimensions of the IMSI block and its components, please refer to Appendix A Figures A1–A3.

Figure 10a shows the 3D design that was imported in Ansys. Figure 10b shows the meshing that was applied on the IMSI block, where the minimum proximity size of the meshing was set to be  $0.003 \text{ m}$ , while its maximum size is  $0.02 \text{ m}$  with a growth rate of  $1.80$  and the total number of elements in the assembly are  $1.75$  million. Figure 10c,d highlights the contact's command, wherein the 'Bonded' command has been used for the block's cavity as the contact and the insulation material as the target body. This command allows the software to treat those bodies as one body that is bonded with no friction or sliding between the parts.



**Figure 9.** SolidWorks assembly of the IMSI block.



**Figure 10.** The setup of the numerical validation. (a) Showing the 3D design in Ansys. (b) Meshing applied on the IMSI block. (c) Using the “bonded” contacts command to define the contact body. (d) Using the “bonded” contacts command to define the target body.

### 3. Results and Discussion

The hot-box experimental unit and numerical model of Ansys are used to simulate and investigate the thermal behavior of an individual IMSI block system. In the current work, the attention is mainly focused on the transfer of heat through a single block system. With

this, the effects of a multi-block system and the possible effects on the thermal performance wherein the blocks are joined using cement and mortar are neglected. As shown in Figure 5, the block is placed such that the right side can be simulated as outside air conditions and the left side as indoor conditions. The experimentation process is conducted using this 'hotbox' setup, and the required temperature measurements are obtained. These measurements are further used to calculate the thermal resistance of the individual block by applying the above-mentioned heat transfer principles and their relevant governing equations.

It is worth noting that four types of studies are conducted to understand and validate the results obtained. These four studies are to investigate the thermal performance of the IMSI block, given as follows:

Study 1: Individual IMSI block system with insulation inserts and without plaster on its surfaces (Experimental).

Study 2: Individual IMSI block system without insulation inserts and without plaster on its surfaces, insulation is replaced by air (Experimental).

Study 3: Individual IMSI block system with insulation inserts and with plaster as a study of the block's usage in real walls of buildings in Bahrain (Experimental).

Study 4: Individual IMSI block system that further validates studies 1 and 3 by simulation through Ansys (Numerical).

Study 5: Individual IMSI block system that investigates the optimization process of the height of the results that are obtained from experiment 4 through Ansys (Numerical).

The following assumptions were considered for all the experiments:

- One-dimensional conduction heat transfer along the x-axis.
- No heat losses take place through the walls of the experimental unit.
- Radiation effects are neglected.
- The effects of the mortar types are neglected.

As mentioned in the results below, the 'hotbox' experimental process involves several steps. However, the accuracy of the obtained results is acceptable. The steady-state thermal conditions are reached in experiment 1, and a clear explanation has been provided for why steady-state conditions were not achieved in experiments 2 and 3. The efforts are conducted to reduce the errors in the results, and a detailed analysis of the IMSI block is conducted as is clear from the four experimental conditions considered. In the future, the obtained test results can be validated using appropriate software tools for the same block, which further can be helpful to propose new designs for the blocks' cavities for improved thermal performance. Eventually, by implementing and observing the difference in the multi-block system, efforts can be made to reduce the energy consumption in the country.

### 3.1. Temperature Measurements, Discussion and Validation

The obtained measurements of temperatures in all the four experiments are presented, discussed, and validated in this section. An instrument named variac is used to maintain the amount of power supplied to the system. For all the experiments, 13% of the variac was maintained which means that only 13% of the total power from the DC supply was provided to the system. This is carried out to ensure the hot outdoor air temperature is within the required range of values for the Kingdom of Bahrain.

#### 3.1.1. Study 1: Individual Block System with Insulation Inserts and without Plaster Using Hot Box (Experimental)

Once the electric current and heater were switched on, the heat gradually flowed thereby orderly increasing the temperature of the hot copper plate, hot air, hot surface of the block, cold surface of the block, and cold air. Three thermocouples were placed on the hot surface and two on the cold surface of the block. The temperature distribution with respect to the time for the steady state to be achieved is presented in Figures 11 and 12, respectively. Through these graphs, an appropriate distribution is presented that shows normal behavior of the rate of heat transfer.

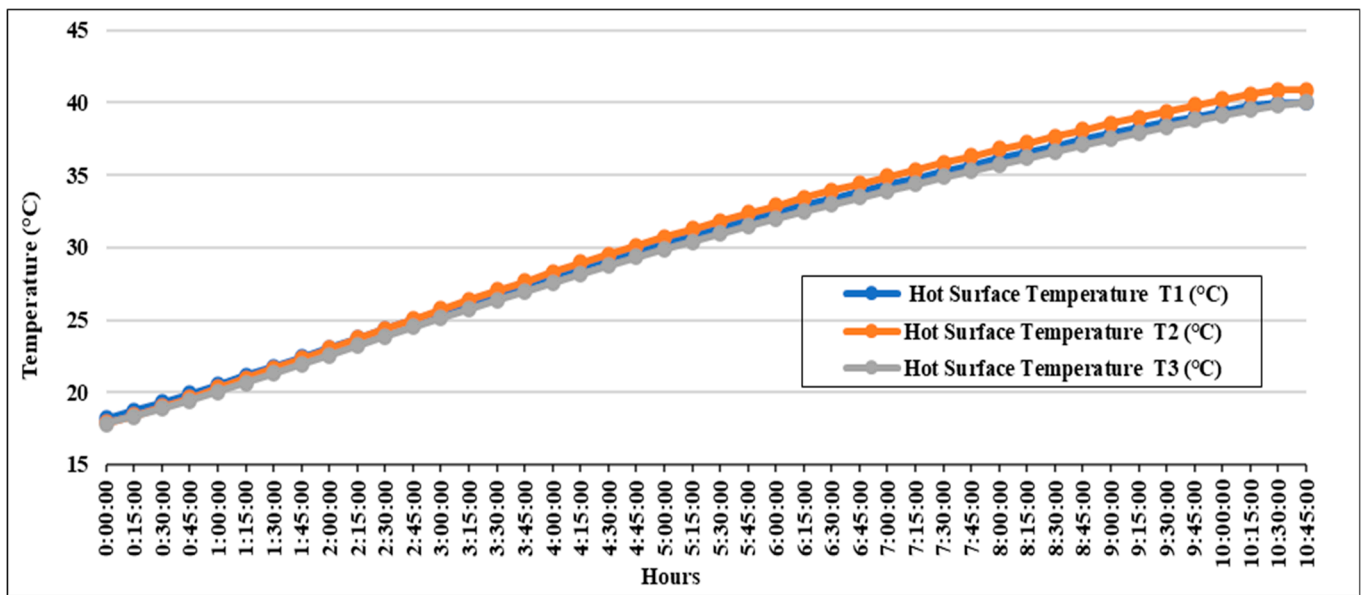


Figure 11. Temperature distribution with respect to time on the hot side of the block.

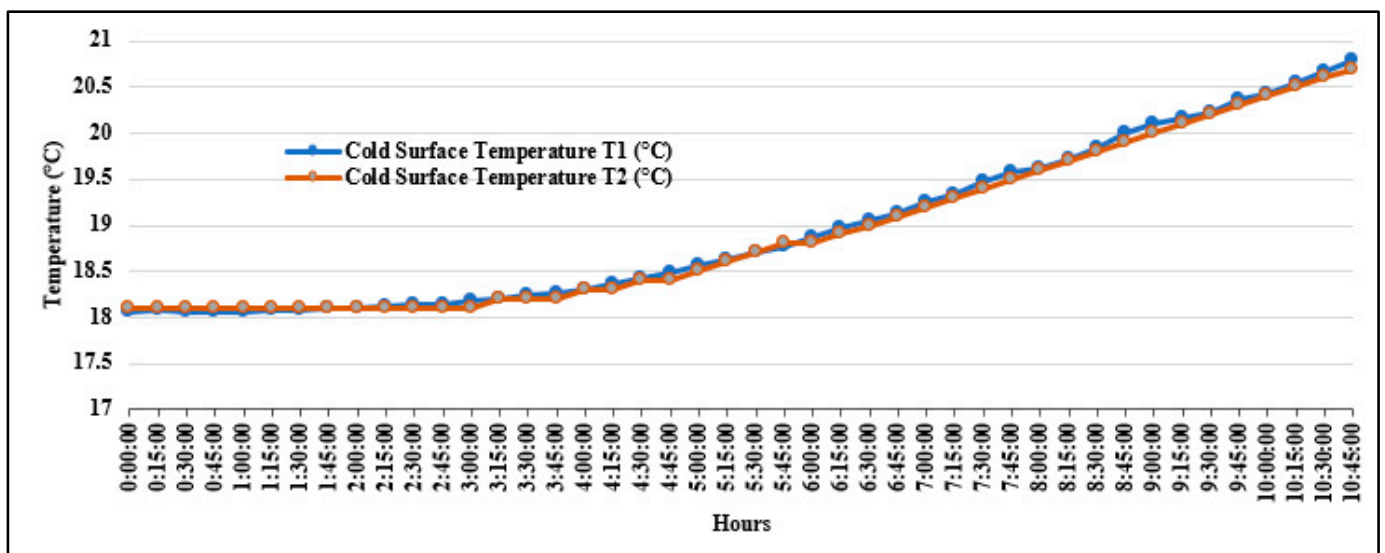


Figure 12. Temperature distribution with respect to time on the cold side of the block.

It can be observed from Figure 13 that initially, all the surfaces are at the same temperatures at 0:00 hrs. After around 10 h 45 min, the temperatures of the surfaces try to stabilize. The difference in the readings as compared with the previous one of 10 h 30 min is as shown in Table 1. It should be noted that each consecutive reading is taken after 15 min, and since the differences are too low, it can be said that the system has reached its steady state condition at 10 h 45 min. The readings at the steady state are in Table 2.

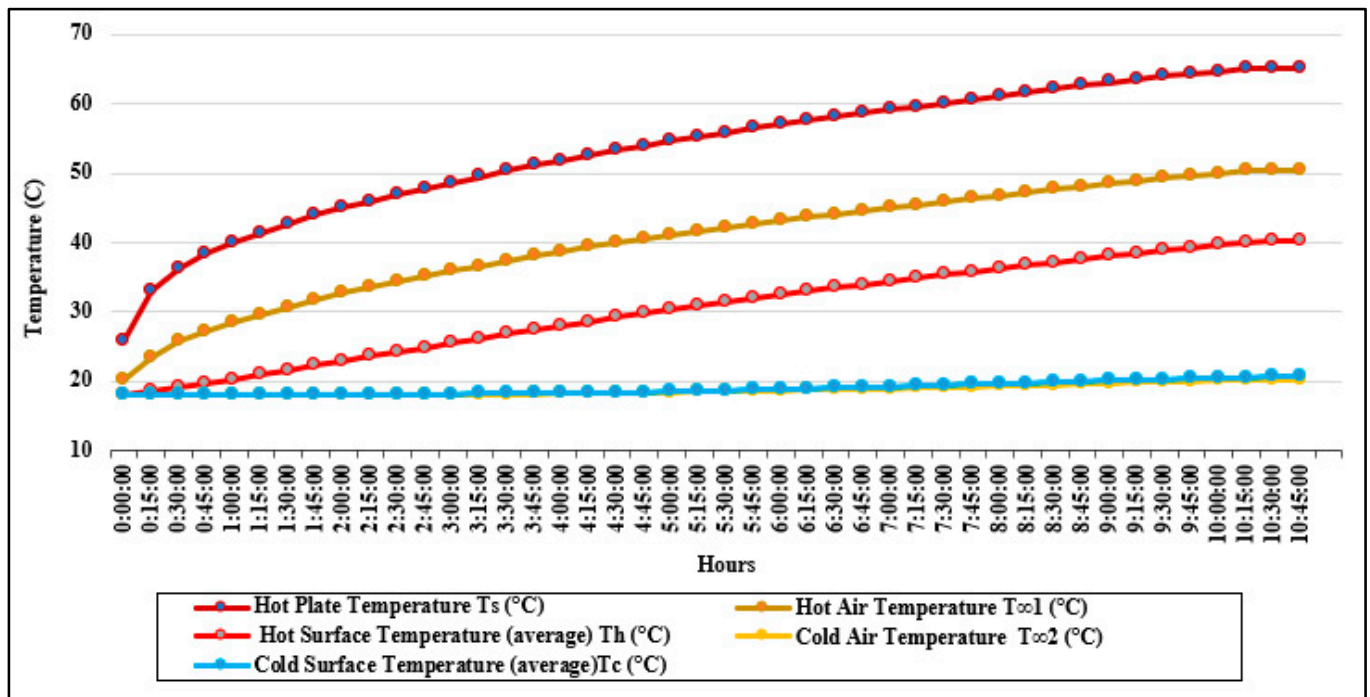


Figure 13. Variation of temperature with respect to time through the IMSI individual block system with insulation inserts and without plaster.

Table 1. Comparison of temperatures at 10:30 h with 10:45 h.

|  |   |
|--|---|
| Hot Plate Temperature $\Delta T_s$             | Hot Air Temperature $\Delta T_{\infty 1}$       |
| 0.02 °C  | 0.002 °C  |
| Hot Surface Temperature (average) $\Delta T_h$ | Cold Surface Temperature (average) $\Delta T_c$ |
| 0.08 °C  | 0.103 °C  |
| Cold Air Temperature $\Delta T_{\infty 2}$     |   |
| 0 °C   |   |

Table 2. Temperatures at steady state condition.

|   |  |
|---|--|
| Hot Plate Temperature $T_s$             | Hot Air Temperature $T_{\infty 1}$       |
| 65.016 °C                               | 50.343 °C                                |
| Hot Surface Temperature (average) $T_h$ | Cold Surface Temperature (average) $T_c$ |
| 40.318 °C                               | 20.741 °C                                |
| Cold Air Temperature $T_{\infty 2}$     |  |
| 20.193 °C                               |  |

The wattmeter indicates the value of the power supplied to the heater. However, to evaluate the thermal resistance of the block, it is important to know the amount of heat contained by the hot air that is in contact with the block. Therefore, the concept of dimensionless numbers is applied to calculate the Grashoff (Gr) number, Rayleigh (Ra) number, and Nusselt (Nu) number based on the properties of air (as shown in Table 3). The governing equations from 1 to 9 (except 4), as well as experimental measurements, are used to evaluate the dimensionless numbers, convection heat transfer coefficient (h), heat flux  $\dot{q}$ , and heat transfer rate (Q) to finally calculate the experimental R-value as shown in Table 4.

**Table 3.** Properties of hot air (uwaterloo.ca, accessed on 15 May 2024).

| Properties of Air at Average of Hot Plate and Hot Air Temperatures (57.68 °C) |  |   |                                     |
|---|--|---|-------------------------------------|
| Density<br>$\rho$ (kg/m <sup>3</sup> )  | Dynamic Viscosity<br>$\mu$ (kg/m s)              | Specific Heat<br>$C_p$ (J/kg K)                     | Thermal Conductivity<br>$k$ (W/m K) |
| 1.0671  | 0.000019956                                      | 1007.9  | 0.028352                            |
| Prandtl Number<br>Pr.No.  | Kinematic Viscosity<br>$\nu$ (m <sup>2</sup> /s) | Thermal Diffusivity<br>$\alpha$ (m <sup>2</sup> /s) | Thermal Expansion<br>$\beta$ (1/K)  |
| 0.70945   | 0.000018701                                      | 0.00002636  | 0.0030227                           |

**Table 4.** Experimental analysis values-R value.

| Dimensionless Numbers |                  |                 | Convective Heat Transfer Coefficient | Heat Flux                     | Heat Transfer Rate | Thermal Resistance of the Block        |
|-----------------------|------------------|-----------------|--------------------------------------|-------------------------------|--------------------|--|
| Grashoff no (Gr)      | Rayleigh no (Ra) | Nusselt no (Nu) | $h$ (W/m <sup>2</sup> K)             | $\dot{q}$ (W/m <sup>2</sup> ) | $Q$ (W)            | R <sub>exp.</sub> m <sup>2</sup> ·°C/W |
| 9,952,754.63          | 7,060,981.775    | 10.56434671     | 497,601,789                          | 21.9743                       | 1.75794            | 0.8909                                 |

*Validation and Error Analysis:*

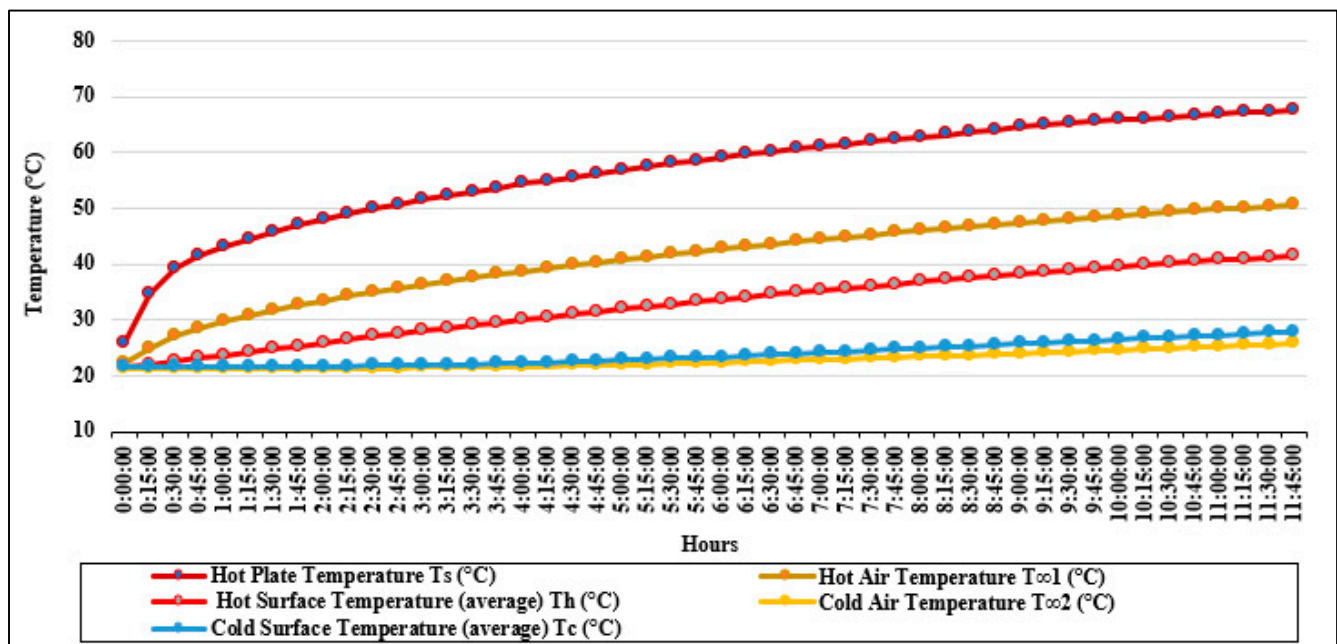
For experiment 1, the validation of the results is made by using the R-value from the block manufacturing company (Appendix A Figure A4) as shown in Table 5 below:

**Table 5.** Thermal resistance of the IMSI individual block system.

| R-Value (Manufacturer)    | R <sub>block,exp</sub> (Experimental) | Deviation |
|---------------------------|---------------------------------------|-----------|
| 0.86 m <sup>2</sup> ·°C/W | 0.8908 m <sup>2</sup> ·°C/W           | 3.59%     |

### 3.1.2. Study 2: Individual Block System without Insulation Inserts and without Plaster Using Hot Box (Experimental)

As Figure 13 of the first experiment, Figure 14 represents the temperatures at each thermocouple inside the hot box throughout the experiment.

**Figure 14.** Variation of temperature with respect to time through IMSI individual block system without insulation inserts and without plaster.

It shows that the temperatures gradually rise with respect to time. However, when Figures 13 and 14 are compared, it is very clear that in Figure 14, in which the insulation inserts are not present, the cold surface and cold air temperatures are different, and unlike Figure 13, in which the insulation inserts are present, they do not overlap each other. It is also noted that after 10 h 30 min, the block with insulation almost reaches a steady-state condition as there are minor variations in the temperatures. However, the block without insulation may require more time to reach a steady-state condition. This is because the air present in the cavities is free to move within the box, which eventually does not allow the system to stabilize. Also, it is worth noticing that at the end of 10 hrs. 45 min, for the same variac percentage, the temperatures of the cold surface (indoor) increase by about 5.529 °C (27.168–21.638 °C) in Figure 14 (without insulation) while in Figure 13 (with insulation), the temperatures of the cold surface (indoor) increase by about 2.66 °C (20.741–18.081 °C). In Figure 14, the increase in the temperature on the cold side is reasonable as there is no insulation installed in the block. Eventually, the effectiveness of the insulation in reducing the rate of heat transfer is noted.

The difference between the hot and cold surfaces of the block is calculated and compared for the block with insulation inserts and the block from which insulation inserts are removed. These values are plotted as shown in Figure 15. It is very clear that the difference in temperatures of the hot and cold surfaces for a block with insulation is higher than that of the block without the insulation inserts for the same variac condition (13%) and same time duration of 10 h 45 min. Hereby, it is validated that insulation plays an important role in reducing the rate of heat transfer through the surface.

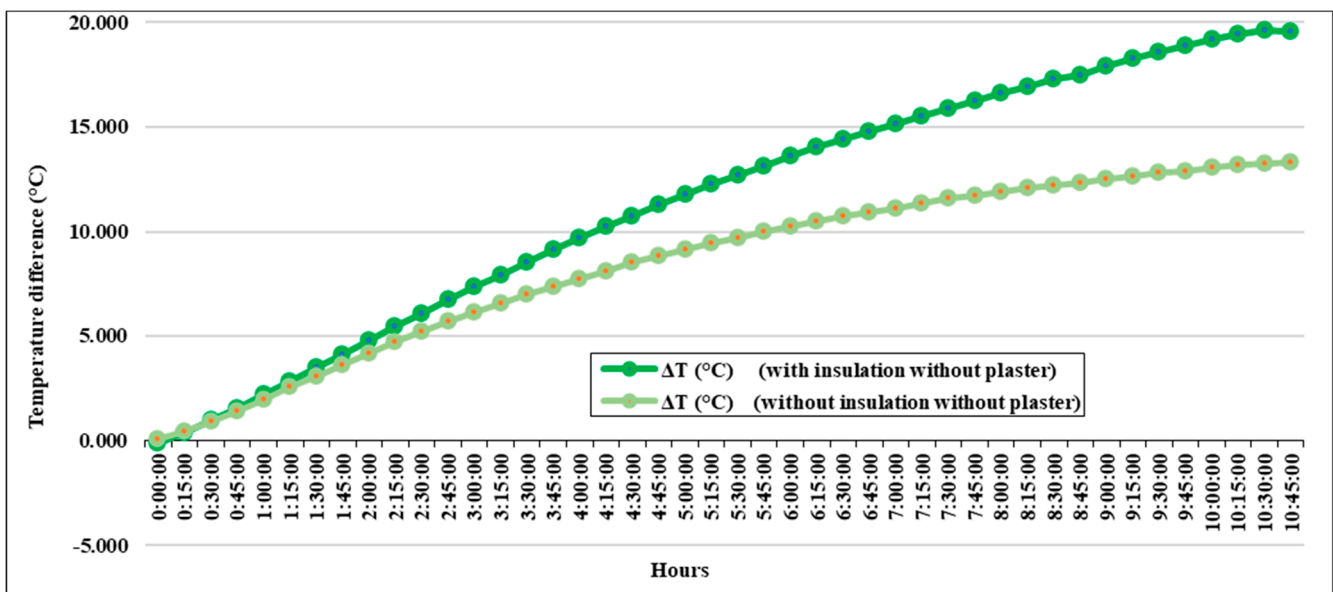


**Figure 15.** Comparison of temperature difference between hot and cold surfaces for blocks with insulation inserts and without insulation inserts.

### 3.1.3. Study 3: Individual Block System with Insulation Inserts and with Plaster Using Hot Box (Experimental)

As Figures 13 and 14 of the first and second experiment, respectively, Figure 16 represents the temperatures at each thermocouple inside the hot box throughout the experiment. It shows that after 12:15 h, the outdoor hot air temperature is 51.727 °C, the average temperature of the hot surface is 44.430 °C, and the average temperature of the cold surface is 24.739 °C. In this experiment, it can be noticed that from 0:00 to 12:15 h, the outdoor air temperature increased by 28.291 °C while on the contrary, the indoor air temperature merely increased by 1.899 °C (24.718–22.819 °C), whereas the first experiment in which plaster is not applied, the indoor air temperature increased by 2.273 °C. Hereby, it



is validated that the plaster of 25 mm on both sides of the block also plays an important role in reducing the rate of heat transfer through the surface.

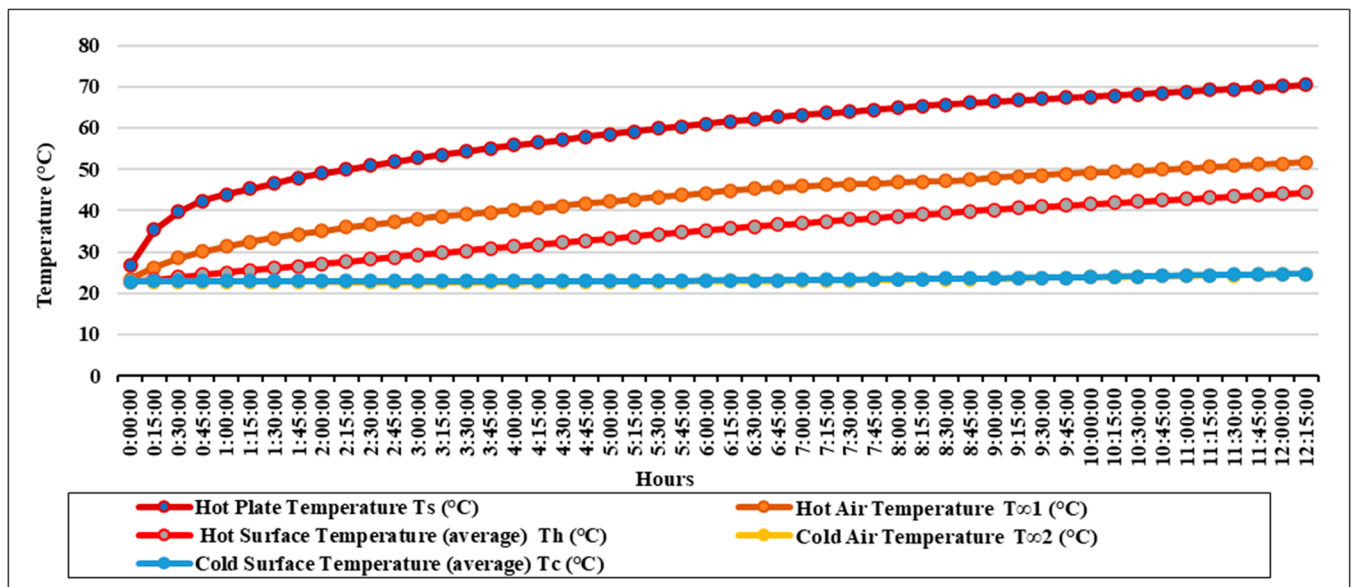


**Figure 16.** Variation of temperature with respect to time through 8'' IMSI individual block system with insulation inserts and with plaster.

It can be observed from Figure 16 that initially, all the surfaces are at the same temperatures at 0:00 hrs. Eventually, once the electric current and heater are switched on, the heat gradually flows through the system, thereby orderly increasing the temperature of the hot copper plate, hot air, hot surface of the block, cold surface of the block, and cold air. Table 6 shows a comparison of temperature variations along layers for all three different conditions of insulation and plaster in the block. After around 10 h 45 min, the difference in the readings as compared with the previous one of 10 h 30 min for the block without plaster and with plaster are shown. For the block without plaster, it should be noted that each consecutive reading is taken after 15 min, and since the differences are too low, we can say that the system reached a steady state-condition at 10 hrs. 45 min. However, for the block with plaster, the readings are a bit on the higher side. Therefore, the experiment was continued, and again, the readings were compared for 12:00 and 12:15 h, which depicts that the system could almost reach a steady state on the hot side, unlike the cold side of the block where the difference of temperatures was a bit higher. Eventually, the setup needed more time to reach a steady-state condition. Due to the limitations of time within the premises, this experiment could not be extended beyond 12:15 h, and since a steady-state condition was not obtained, it was not possible to calculate the R-value of the block. However, the effectiveness of the plaster can be clearly observed in the temperature variations.

**Table 6.** Comparison of temperature variations along different layers of setup for different conditions of the block.

| Different Conditions of Insulation and Plaster                  | With Insulation Without Plaster | With Insulation With Plaster    | With Insulation With Plaster    |
|---|---------------------------------|---------------------------------|---------------------------------|
| Variations in temperatures across different layers of the setup | comparison at 10:30 and 10:45 h | comparison at 10:30 and 10:45 h | comparison at 12:00 and 12:15 h |
| Hot Plate Temperature $\Delta T_s$                              | 0.02 °C                         | 0.326 °C                        | 0.326 °C                        |
| Hot Air Temperature $\Delta T_{\infty 1}$                       | 0.002 °C                        | 0.294 °C                        | 0.27 °C                         |
| Hot Surface Temperature (average) $\Delta T_h$                  | 0.08 °C                         | 0.32 °C                         | 0.293 °C                        |
| Cold Surface Temperature (average) $\Delta T_c$                 | 0.103 °C                        | 0.094 °C                        | 0.112 °C                        |
| Cold Air Temperature $\Delta T_{\infty 2}$                      | 0 °C                            | 0.098 °C                        | 0.11 °C                         |

### 3.1.4. Study 4: Numerical Results

Numerical analysis was conducted for studies 1 and 3, which are discussed in this section.

#### *Individual Block System with Insulation Inserts without Plaster Using Ansys (Numerical):*

This numerical study is conducted through simulation by using Ansys as a tool to further validate the results and compare it with the experimental and manufacturer's values. The sides of the IMSI block in the simulation are perfectly insulated, and the input parameters are included in the front and back surfaces, which are directly perpendicular to the heat flow. The average values from the experimental results are considered for this experiment and used as input parameters for the simulation. The parameters: 'Cold Temperature ( $T_C$ )' as 20.741 °C and the 'Heat Flux ( $q$ )' as 21.974 W/m<sup>2</sup> were entered as the input parameters for the simulation. The cold temperature is applied on the cold side, and the heat flux value is plugged in from the hot side in accordance with the setup of the hotbox experiment, which helped to obtain the hot surface temperature value as the output. Hence, it was possible to calculate the  $R_{\text{block,num.}}$  of the IMSI block using Equation (4). Figures 17 and 18 highlight the simulation results of the distribution of temperature from, respectively, the hot side and cold side of the IMSI block with insulation inserts and without plaster.

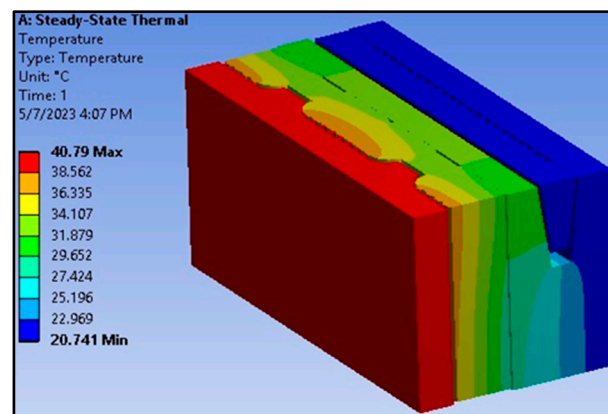


**Figure 17.** Simulation results of the IMSI block with no plaster (hot side).

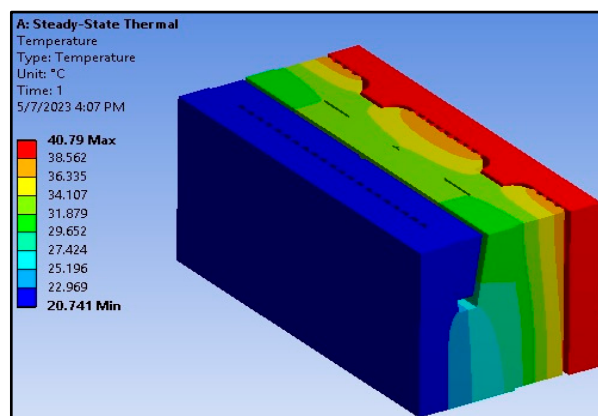


**Figure 18.** Simulation results of the IMSI block with no plaster (cold side).

#### *Validation and Error Analysis:*

After conducting the simulation, it was noted that the value of hot temperature  $T_{h,num}$  (Numerical) was 40.79 °C. While the value of hot temperature from experimental method  $T_{h,exp}$  (Experimental) was 40.318 °C. Eventually, the deviation between these values turned out to be 1.171%.

Moreover, the  $R_{\text{block,num.}}$  of the numerical approach was evaluated by applying the thermal resistance Equation (4), which turned out to be 0.9124 m<sup>2</sup>·°C/W. While the

$R_{\text{block,exp}}$ . (Experimental) from Table 4 was  $0.8908 \text{ m}^2 \cdot \text{°C}/\text{W}$ . Upon comparison between the numerical and experimental R-values of the IMSI block, a deviation of 2.411% was observed. Also, upon comparison between the numerical and manufacturer's R-values of the IMSI block, a deviation of 5.743% was observed.

The deviations of R-values of numerical vs. experimental and numerical vs. manufacturer's can be justified by considering many reasons that can affect the output of the analysis. It is worth noting that there was no official engineering drawing of the block provided by the manufacturer, and therefore, the dimensions of the IMSI block were taken manually using a measuring tape and a vernier caliper. Secondly, the numerical method considered that the insulation and concrete layers of the IMSI block are perfectly insulated with no heat loss, while in a real block, some gaps do exist between these layers. However, it is believed that the meshing that was applied to the IMSI block was satisfactory. Thirdly, the thermal conductivity of the materials of the block was determined by going through the literature and choosing the appropriate value. Meaning that there is no specific value from the manufacturer to determine the material property of the IMSI block. Finally, the R-value from the manufacturer is based on the laboratory test (Appendix A Figure A4) conducted in a controlled environment with 0% humidity, which can be one of the reasons for the deviation. Eventually, it is observed that since fair and appropriate measures were taken to simulate the experimental and numerical analysis, satisfactory results were obtained with an acceptable error percentage.

*Individual Block System with Insulation Inserts with Plaster Using Ansys (Numerical):*

An external plaster of 25 mm on the inner and outer surface of the IMSI block is applied in accordance with the guidelines provided by the Electricity and Water Authority (EWA) of Bahrain. The input parameters for this numerical investigation are the same as the previously mentioned values (the cold side was set as  $20.741 \text{ °C}$ , and the heat flux set on the hot side of the blocks was  $21.974 \text{ W}/\text{m}^2$ ). However, the thermal conductivity of the external plaster in this simulation will be considered, which is  $0.08 \text{ W}/\text{m K}$  [33]. The sides of the IMSI block with plaster are perfectly insulated with the "bonded" contacts command being applied between its parts and between the plastering, as well, to identify it as one body with no gap, sliding, or friction in between. Further, the effect of applying the plaster on the thermal resistance of the block was analyzed.

Figures 19 and 20 highlight the simulation results of the distribution of temperature from the hot side and cold side of the IMSI block, respectively, with insulation inserts and with plaster.

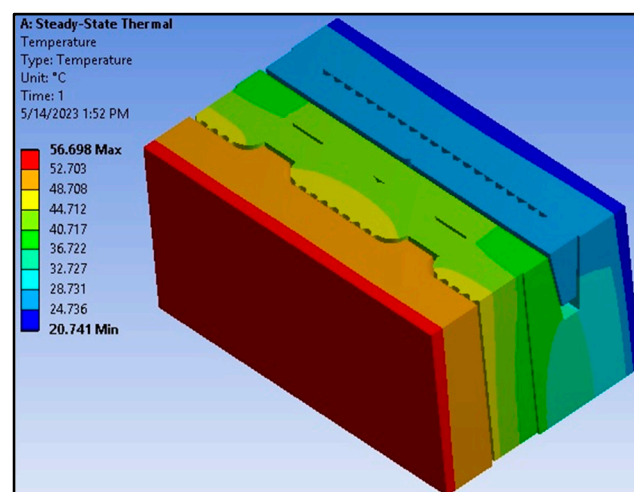


**Figure 19.** Simulation results of the IMSI block with plaster (hot side).

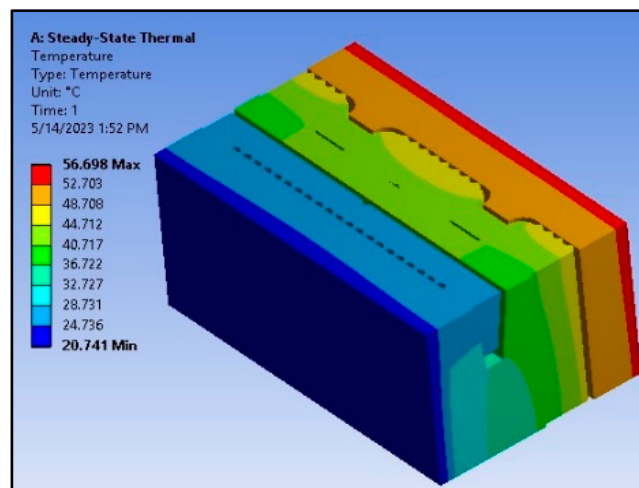


**Figure 20.** Simulation results of the IMSI block with plaster (cold side).

#### Validation and Error Analysis:

The R-values of the IMSI block using the numerical method with plaster  $R_{\text{block,num. (Plaster)}}$  is  $1.6363 \text{ m}^2 \cdot \text{°C}/\text{W}$  while without plaster  $R_{\text{block,num. (No Plaster)}}$  (from experiment 4) is  $0.9124 \text{ m}^2 \cdot \text{°C}/\text{W}$ , respectively. Therefore, it is noted that the R-value of the IMSI block where the external plaster is applied has been improved by 79.34%.

Figure 21 shows an important part and comparative study of the overall research work. Starting with the manufacturer's value from Bahrain blocks without plaster, this value is referenced from the manufacturer as  $0.86 \text{ m}^2 \cdot \text{°C}/\text{W}$ , while the experimental value using hot box was  $0.8909 \text{ m}^2 \cdot \text{°C}/\text{W}$ , thereby showing a deviation of 3.59%.

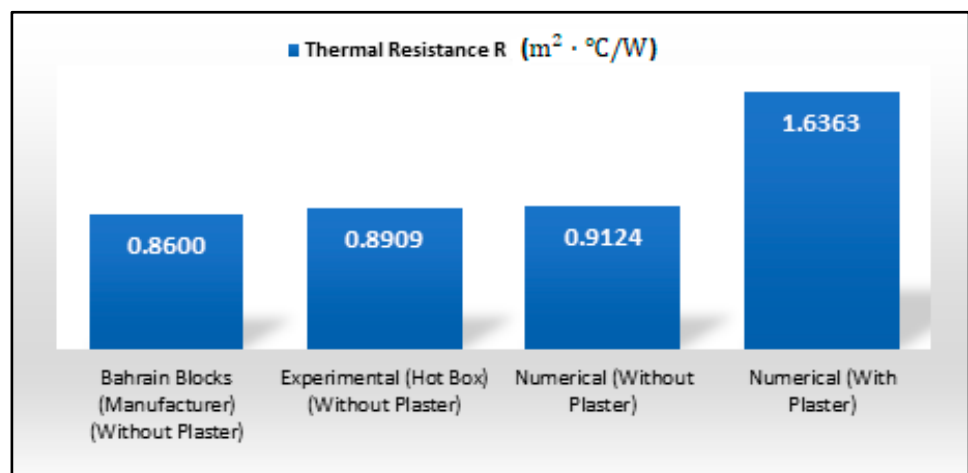


**Figure 21.** A graph showing the block types and their corresponding R-values.

Moreover, when attempting to numerically validate the thermal resistance of the IMSI block in a condition where no external plaster was applied, it was noted that the thermal resistance of the block was  $0.9124 \text{ m}^2 \cdot \text{°C}/\text{W}$ . Hence, resulting in a deviation of 2.367% between the numerical, and experimental value, and a deviation of 5.743% when compared with the manufacturer's value. Furthermore, when applying the external plaster to the numerical study of the IMSI block under the same meshing and parameter conditions then, an improvement of 79.34% in thermal performance was observed with the thermal resistance (R-value) to be  $1.6363 \text{ m}^2 \cdot \text{°C}/\text{W}$ . This confirms the effectiveness of the external plaster and its major improvement for the thermal resistance.

### 3.1.5. Study 5: Optimization of the Height of Insulation of the Single Block, with and without Plaster

As per the regulations of EWA, the overall dimensions of the block are constant. Accordingly, an 8" block must be of 400 mm × 200 mm × 200 mm overall dimensions. Therefore, optimization could be made only in the design of the two insulation inserts—the front and the rear. This could include the insulation's height or thickness or both. However, to begin with, it was decided to optimize the height of the rear insulation insert because of the simplicity of its design. The optimization process was conducted under the same simulation settings as the previous numerical experiment on the single block (study 4) to investigate the corresponding thermal resistance due to the change in the height of the rear insulation.

Figure 22 shows the geometry of the rear insulation that was optimized where the height of both ends of the rear insulation was gradually increased. This was to investigate the effect of the change in the insulation's height on the thermal resistance of the IMSI block. Figure 23 shows the original condition of the block, where it has 85 mm of depth into the cavity with a gap for air and the maximum optimization of 30 mm increment in its height, resulting in a total height of 115 mm with no gap for air. Hence, removing concrete material from the cavity and replacing it with expanded polystyrene.

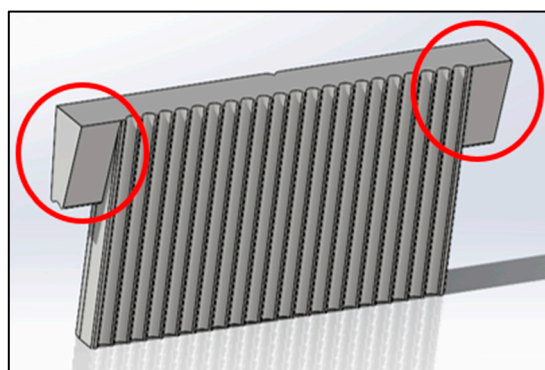


Figure 22. Highlighting the geometry that is optimized.

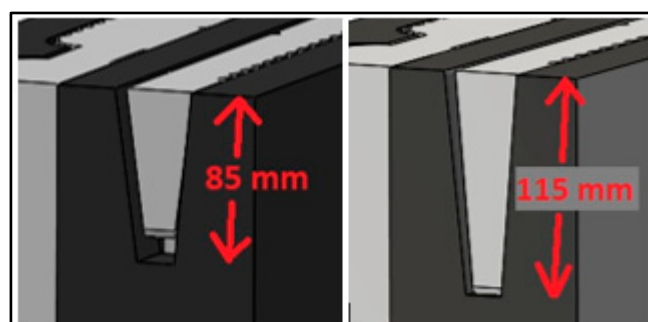


Figure 23. Showing the difference between the original, and optimized version of the back insulation insert and cavity.

This way, the optimization was conducted for four different conditions as shown in Table 7. In condition 1, the air gap was filled with insulation, while for conditions 2, 3, and 4, the height of the insulation was increased by 20 mm, 25 mm, and 30 mm, respectively. It should be noted that in conditions 2, 3, and 4, where the insulation height was increased, a correspondingly equivalent quantity of concrete was removed from the block. Further, numerical analysis was conducted for all the above four cases while keeping the same input conditions as in study 4 wherein the temperature on the cold side was set as 20.741 °C, and the heat flux set on the hot side of the blocks was 21.974 W/m<sup>2</sup>. The results obtained for the block without plaster and with plaster are presented in Tables 8 and 9, respectively.

The last column in Table 8 shows the improvement in the R-value in % when compared with the manufacturer's value of  $0.86 \text{ m}^2 \cdot ^\circ\text{C}/\text{W}$ . While the last column in Table 9 shows the improvement in the R-value in % when compared with the value of  $1.6363 \text{ m}^2 \cdot ^\circ\text{C}/\text{W}$  obtained through numerical analysis in study 4 for a block with plaster. This is because of the unavailability of test reports for blocks with plaster as the manufacturers do not conduct such type of testing.

**Table 7.** Different optimization conditions.

| Optimization of the Back Insulation Insert |                            |
|--|----------------------------|
| Condition 1                                | Gap filled with insulation |
| Condition 2                                | +20 mm insulation          |
| Condition 3                                | +25 mm insulation          |
| Condition 4                                | +30 mm insulation          |

**Table 8.** Showing the improvement from optimization on the block without plaster.

| Block Thermal Resistance (Without Plaster) |                            |  |         |
|--|----------------------------|--|---------|
| Condition                                  | $T_h$ ( $^\circ\text{C}$ ) | R ( $\text{m}^2 \cdot ^\circ\text{C}/\text{W}$ ) | R (%)   |
| Original                                   | 40.79                      | 0.9124   | 6.0926  |
| Filled                                     | 40.771                     | 0.9115   | 5.9921  |
| +20 mm                                     | 42.721                     | 1.0003   | 16.3108 |
| +25 mm                                     | 43.329                     | 1.0279   | 19.5282 |
| +30 mm                                     | 43.996                     | 1.0583   | 23.0577 |

**Table 9.** Showing the improvement from optimization on the block with plaster.

| Block Thermal Resistance (With Plaster) |                            |  |         |
|---|----------------------------|--|---------|
| Condition                               | $T_h$ ( $^\circ\text{C}$ ) | R ( $\text{m}^2 \cdot ^\circ\text{C}/\text{W}$ ) | R (%)   |
| Original                                | 56.698                     | 1.6363   | 72.3946 |
| Filled                                  | 56.666                     | 1.6349   | 72.3355 |
| +20 mm                                  | 59.019                     | 1.7420   | 74.1695 |
| +25 mm                                  | 59.745                     | 1.7750   | 74.7065 |
| +30 mm                                  | 60.535                     | 1.8110   | 75.2662 |

#### Validation:

In Figure 24, the results of the thermal resistances obtained from both Tables 8 and 9 are plotted, where the blue bars represent the values without plaster and the orange bars with plaster for the four optimized conditions, along with the results of the original block. It was noted that the thermal resistance gradually increased with the increase in the height of the insulation for both with and without plaster situations.

Also, as seen in the figure, a gradual increase in the thermal resistance with respect to the increase in the height of the rear insulation was observed. The values of the thermal resistance of the original block without plaster and with plaster were  $0.9124 \text{ m}^2 \cdot ^\circ\text{C}/\text{W}$  and  $1.6363 \text{ m}^2 \cdot ^\circ\text{C}/\text{W}$ , respectively, which increased to  $1.0583 \text{ m}^2 \cdot ^\circ\text{C}/\text{W}$  and  $1.8110 \text{ m}^2 \cdot ^\circ\text{C}/\text{W}$ , respectively, at its maximum optimized condition of +30 mm.

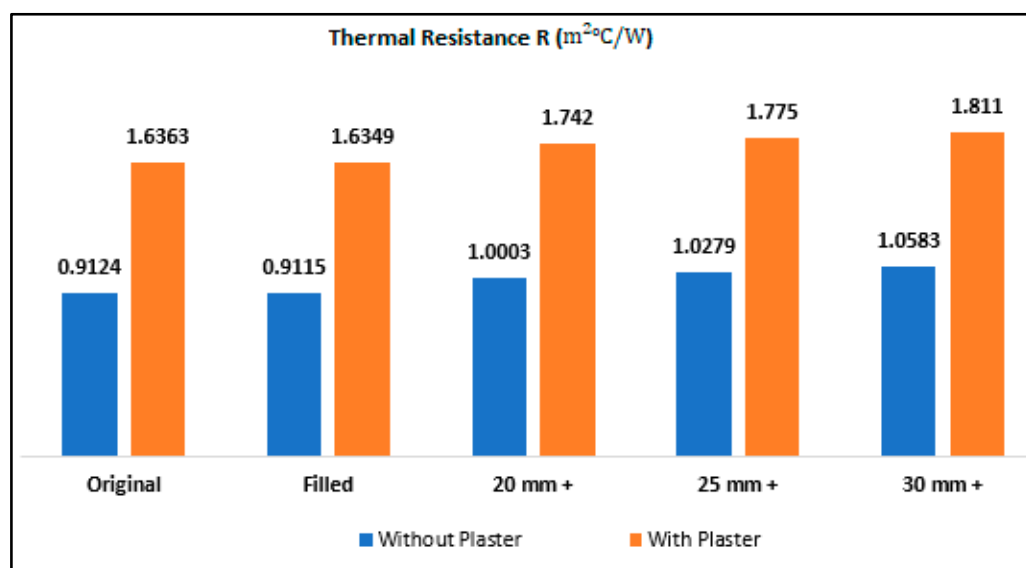


Figure 24. Plotting the obtained results of the optimization process.

#### 4. Conclusions

The primary focus of this study was the thermal assessment of individual blocks in a controlled setting, both experimentally and numerically. In the present work, results and analyses for five studies on an individual IMSI block were presented. The experimental approach for studies 1, 2, and 3 used the hot box method, while the numerical approach for studies 4 and 5 employed the finite element method (FEM) using Ansys software.

The first three studies examined the impact of plaster and insulation inserts on the block's thermal performance, while the fourth study validated these results with less than 6% deviations. To date, no study has been conducted to observe the effect of plaster on the R-value of the IMSI block. From the current study, it was observed that the plaster improves the block's R-value by 79.34%. Further, Ansys thermal steady-state analysis effectively illustrated the temperature distribution through the block. Additionally, optimizing the height of the block's rear insulation insert by 30 mm increased the R-value by 10.67%, a modest but significant improvement.

The optimization process in study 5 worked on increasing the height of the rear insulation. However, this was achieved by the removal of an equivalent amount of the concrete material and replacing it with expanded polystyrene. The deduction of the concrete material might affect the mechanical strength of the IMSI block. As this study only investigates the effect of the optimization process on the thermal resistance, in the future, more investigation must be conducted on the mechanical strength of the IMSI block and its ability to withstand the load after the optimization process. Moreover, this study was mainly focused on individual block systems. Whereas, in reality, buildings are made of walls that constitute multiple blocks that are joined together using mortar layers. Studies are required to understand how these interactions affect overall thermal performance in multi-block configurations. It is necessary to investigate whether the principles observed in single blocks hold true when applied to larger, more complex assemblies. This work estimates thermal resistance under steady-state conditions, which do not account for the dynamic thermal loads that building blocks experience in real-world scenarios. Research is needed to incorporate dynamic thermal loads and assess their impact on thermal resistance.

**Author Contributions:** Conceptualization, P.A.M. and A.M.M.; Methodology, A.M.M.; Software, A.E.A.; Validation, A.M.M. and Y.A.A.; Formal analysis, P.A.M. and A.E.A.; Investigation, Y.A.A.; Data curation, P.A.M.; Writing—original draft, P.A.M.; Supervision, A.M.M. and Y.A.A. All authors have read and agreed to the published version of the manuscript.

**Funding:** This research received no external funding.

**Data Availability Statement:** Data are contained within the article.

**Conflicts of Interest:** The authors declare no conflict of interest.

## Appendix A

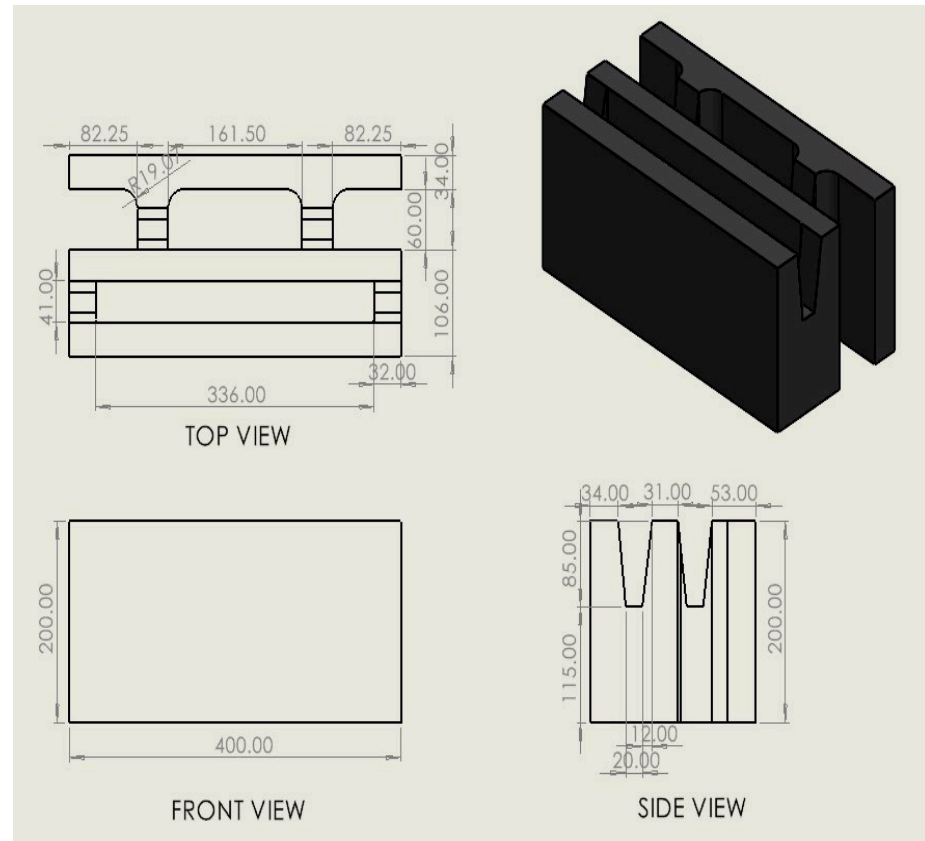


**Figure A1.** Showing the major dimensions in the concrete block.

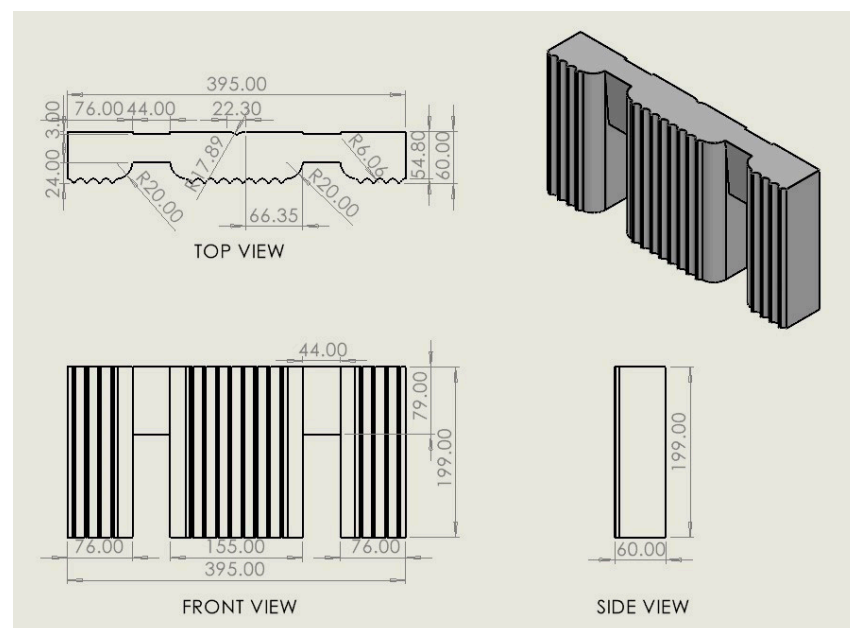


**Figure A2.** Showing the major dimensions in the front insulation.



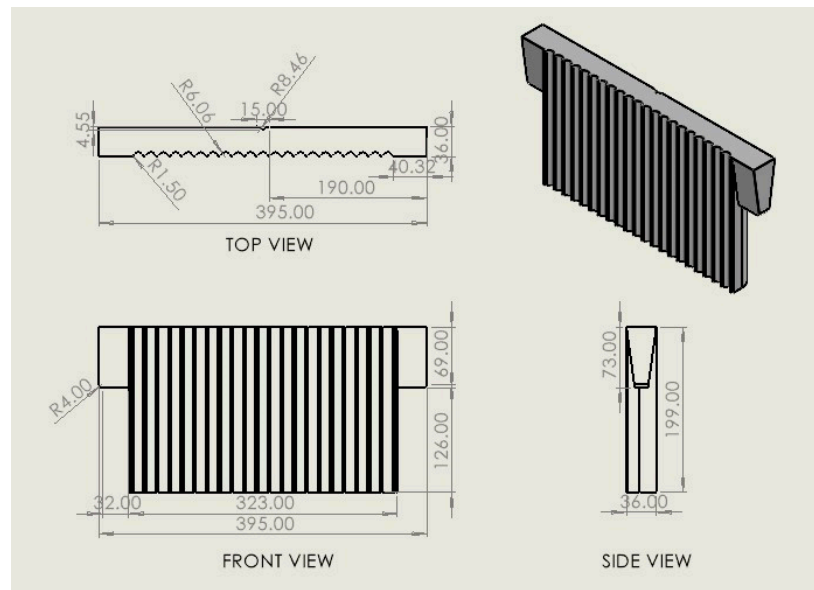


Figure A3. Showing the major dimensions in the back insulation.

| LABORATORY TEST REPORT<br>THERMAL TRANSMISSION PROPERTIES BY HEAT FLOW METER   |                       | Reference: MED-CRS-F-032                           |  |
|--|-----------------------|--|--|
|  |                       | Rev: 0   |  |
| <b>TEST RESULTS:</b>   |                       |  |  |
| Parameters   | Results               | Units  |  |
| Concrete Density   | 2410                  | Kg/m <sup>3</sup>                                  |  |
| Expanded Polystyrene Density   | 19.59                 | Kg/m <sup>3</sup>                                  |  |
| Mean Temperature   | 35°                   | C°   |  |
| Δ Temperature  | 30°                   | C°   |  |
| <b>Non-Dry Test</b>  |                       |  |  |
| <b>Specimen 1</b>  |                       |  |  |
| Relative Humidity (RH)   | 60±5                  | %  |  |
| Thickness  | 200.4                 | mm   |  |
| Tested Specimen Dimensions   | 600*400               | mm   |  |
| Thermal Conductivity (λ)   | 0.232                 | W/m.k  |  |
| Thermal Resistance (R)   | 0.85                  | m <sup>2</sup> .k/W                                |  |
| Thermal Transmittance (U)  | 1.16                  | W/m <sup>2</sup> .k                                |  |
| Heat Flux (q)  | 33.69                 | W/m <sup>2</sup>                                   |  |
| Test Duration  | 854                   | min.   |  |
| <b>Dry Test</b>  |                       |  |  |
| <b>Specimen 2</b>  |                       |  |  |
| Relative Humidity (RH)   | 0%                    | %  |  |
| Thickness  | 200.3                 | mm   |  |
| Tested Specimen Dimensions   | 600*400               | mm   |  |
| Thermal Conductivity (λ)   | 0.208                 | W/m.k  |  |
| Thermal Resistance (R)   | 0.96                  | m <sup>2</sup> .k/W                                |  |
| Thermal Transmittance (U)  | 1.04                  | W/m <sup>2</sup> .k                                |  |
| Heat Flux (q)  | 30.27                 | W/m <sup>2</sup>                                   |  |
| Test Duration  | 837                   | min.   |  |
| <b>Comments/Disclaimer:</b>  |                       |  |  |
| <ul style="list-style-type: none"> <li>This Report is valid for maximum of <b>2 year(s)</b> from the date of this Report unless otherwise stated or there is a change / revision in the material technical specifications, manufacturing process or relevant Standards &amp; Specifications requirements.</li> <li>The test report relates only to the sample tested. MED shall not be liable for any changes in reported factual data due to any cause related to sample tested after the report, in respect of it, has been issued.</li> </ul> |                       |  |  |
|  | <b>Reported by</b>    | <b>Reviewed by</b>                                 | <b>Approved by</b>                       |
| <b>Name:</b>   | Ahmed Al-Hadi         | Abdul Aziz Johari                                  | Raed Ahmad Ibrahim                       |
| <b>Title:</b>  | Senior Civil Engineer | Head, Architectural<br>Materials Consultancy Group | Chief, Consultancy &<br>Research Section |
| <b>Date:</b>   | Oct-02-2019           | Oct-02-2019  | Oct-02-2019                              |
| <b>Signature:</b>  |                       |  |  |
| <small>P.O. Box 5, Mamama, Kingdom of Bahrain, Juffair, Building 1221, Road 4226, Block 342, Tel: 17812444, Fax: 17812445, Email: info@medcrs.com</small><br><small>Web: www.medcrs.com.bh</small>   |                       |  |  |
| <small>Note: This Report Contains 2 Pages</small>  |                       |  |  |

Figure A4. A copy of the laboratory test report on the individual IMSI block from Bahrain blocks.

## References

1. Chel, A.; Kaushik, G. Renewable energy technologies for sustainable development of energy efficient building. *Alex. Eng. J.* **2018**, *57*, 655–669. [\[CrossRef\]](#)
2. Cao, X.; Dai, X.; Liu, J. Building energy-consumption status worldwide and the state-of-the-art technologies for zero-energy buildings during the past decade. *Energy Build.* **2016**, *128*, 198–213. [\[CrossRef\]](#)
3. Akkurt, G.G.; Aste, N.; Borderon, J.; Buda, A.; Calzolari, M.; Chung, D.; Costanzo, V.; Del Pero, C.; Evola, G.; Huerto-Cardenas, H.E.; et al. Dynamic thermal and hygrometric simulation of historical buildings: Critical factors and possible solutions. *Renew. Sustain. Energy Rev.* **2020**, *118*, 109509. [\[CrossRef\]](#)
4. Martinez, S.; Singh, P. Thermal Performance of Roof Structures and Their Interaction with Wall Insulation. *Energy Build.* **2019**, *180*, 55–67. [\[CrossRef\]](#)
5. Cho, K.; Cho, D.; Koo, B.; Yun, Y. Thermal Performance Analysis of Windows, Based on Argon Gas Percentages between Window Glasses. *Buildings* **2023**, *13*, 2935. [\[CrossRef\]](#) [\[PubMed\]](#)
6. Rana, A.; Alam, M.S.; Charles, K.; Kaluthantirige, P.P.; Hewage, K.; Sadiq, R. Thermal performance of double and triple glazed windows Experimental results from lab and in-situ measurements. In Proceedings of the 1st International Conference on New Horizons in Green Civil Engineering (NHICE-01), Victoria, BC, Canada, 25–27 April 2018.
7. Al-Abduljabbar, A.; Al-Mogbel, M.; Danish, S.N.; El-Leathy, A. Insulation Performance of Building Components and Effect on the Cooling Load of Homes in Saudi Arabia. *Sustainability* **2023**, *15*, 5685. [\[CrossRef\]](#) [\[PubMed\]](#)
8. Sustainable Energy for All, Building Efficiency Accelerator. 2015. Available online: <https://www.seforall.org/partners/building-efficiency-accelerator> (accessed on 15 May 2024).
9. World Bank. *Kingdom of Bahrain Energy Efficiency Program (KEEP)*; World Bank: Washington, DC, USA, 2016.
10. *Annual Report 2018*; MEW (Ministry of Electricity and Water): Manama, Bahrain, 2018.
11. World Data Atlas, Bahrain Energy. 2019. Available online: <https://knoema.com/atlas/Bahrain/Primary-energy-consumption#:~:text=In%202019,%20primary%20energy%20consumption,average%20annual%20rate%20of%203.14%25> (accessed on 24 April 2024).
12. Alnaser, N. Building integrated renewable energy to achieve zero-emission in Bahrain. *Energy Build.* **2015**, *93*, 32–39. [\[CrossRef\]](#)
13. Mahdaoui, M.; Hamdaoui, S.; Msaad, A.A.; Kousksou, T.; El Rhafiki, T.; Jamil, A.; Ahachad, M. Building bricks with phase change material (PCM): Thermal performances. *Constr. Build. Mater.* **2020**, *269*, 121315. [\[CrossRef\]](#)
14. Kishore, R.A.; Bianchi, M.V.; Booten, C.; Vidal, J.; Jackson, R. Optimizing PCM-integrated walls for potential energy savings in U.S. Buildings. *Energy Build.* **2020**, *226*, 110355. [\[CrossRef\]](#)
15. Iffa, E.; Tariku, F.; Simpson, W.Y. Highly Insulated Wall Systems with Exterior Insulation of Polyisocyanurate under Different Facer Materials: Material Characterization and Long-Term Hygrothermal Performance Assessment. *Materials* **2020**, *13*, 3373. [\[CrossRef\]](#) [\[PubMed\]](#)
16. Shanmuham, T.S.S.; Nguyen, P.T.T.; Do, N.H.; Le, D.K.; Thai, Q.B.; Le, P.K.; Phan-Thien, N.; Duong, H.M. Advanced fabrication and multi-properties of aluminium hydroxide aerogels from aluminium wastes. *J. Mater. Cycles Waste Manag.* **2021**, *23*, 885–894. [\[CrossRef\]](#)
17. Al-Tamimi, A.S.; Al-Amoudi, O.S.B.; Al-Osta, M.A.; Ali, M.R.; Ahmad, A. Effect of insulation materials and cavity layout on heat transfer of concrete masonry hollow blocks. *Constr. Build. Mater.* **2020**, *254*, 119300. [\[CrossRef\]](#)
18. Ghailane, H.; Ahamat, M.A.; Padzi, M.M.; Beddu, S. Steady-state heat flow through hollow clay bricks. *Mater. Sci. Eng.* **2019**, *834*, 012021. [\[CrossRef\]](#)
19. Cuce, E.; Cuce, P.; Besir, A. Improving thermal resistance of lightweight concrete hollow bricks: A numerical optimisation research for a typical masonry unit. *J. Energy Syst.* **2020**, *4*, 121–144. [\[CrossRef\]](#)
20. Shehata, N.; Sayed, E.; Abdelkareem, M. Recent progress in environmentally friendly geopolymers: A review. *Sci. Total Environ.* **2020**, *762*, 143166. [\[CrossRef\]](#)
21. Ashraf, N.; Nasir, M.; Al-Kutti, W.; Al-Maziad, F. Assessment of thermal and energy performance of masonry blocks prepared with date palm ash. *Mater. Renew. Sustain. Energy* **2020**, *9*, 17. [\[CrossRef\]](#)
22. Zhang, Q.; Mao, S. Investigation of the bond strength and microstructure of the interfacial transition zone between cement paste and aggregate modified by Bayer red mud. *J. Hazard. Mater.* **2021**, *403*, 123482. [\[CrossRef\]](#)
23. Al-Awsh, W.A.; Qasem, N.A.A.; Al-Amoudi, O.S.B.; Al-Osta, M.A. Experimental and numerical investigation on innovative masonry walls for industrial and residential buildings. *Appl. Energy* **2020**, *276*, 115496. [\[CrossRef\]](#)
24. Martinez, L.; Wang, K. Infrared Thermography for In-Situ Measurement of Thermal Performance of Building Envelopes. *Energy Build.* **2018**, *158*, 51–60. [\[CrossRef\]](#)
25. Alqahtani, S.; Ali, H.M.; Ali, H.; Farukh, F.; Kandan, K. Development of affordable hot box calorimeter to determine the U-value of inhomogeneous building material. *J. Mater. Res. Technol.* **2023**, *25*, 6492–6502. [\[CrossRef\]](#)
26. Patel, S.; Nguyen, T. Evaluation of Thermal Resistance of Sustainable Building Materials Using Heat Flow Meter Method. *J. Sustain. Archit. Civ. Eng.* **2020**, *26*, 35–48.
27. Faraji, M. Numerical study of the thermal behavior of a novel Composite PCM/concrete wall. *Energy Procedia* **2017**, *139*, 105–110. [\[CrossRef\]](#)
28. Kanellopoulos, G.; Koutsomarkos, V.G.; Kontoleon, K.J.; Georgiadis-Filikas, K. Numerical Analysis and Modelling of Heat Transfer Processes through Perforated Clay Brick Masonry Walls. *Procedia Environ. Sci.* **2017**, *38*, 492–499. [\[CrossRef\]](#)

29. Sassine, E.; Cherif, Y.; Dgheim, J.; Antczak, E. Experimental and Numerical Thermal Assessment of Lebanese Traditional Hollow Blocks. *Int. J. Thermophys.* **2020**, *41*, 47. [[CrossRef](#)]
30. Domínguez-Muñoz, F.; Anderson, B.; Cejudo-López, J.M.; Carrillo-Andrés, A. Uncertainty in the thermal conductivity of insulation materials. *Energy Build.* **2010**, *42*, 764–772. [[CrossRef](#)]
31. Radhi, H.; Sharples, S.; Taleb, H.; Hafmy, M. Will cool roofs improve the thermal performance of our built environment? A study assessing roof systems in Bahrain. *Energy Build.* **2016**, *135*, 324–337. [[CrossRef](#)]
32. Modi, P.; Bushehri, R.; Georgantopoulou, C.; Mavromatidis, L. Design and development of a mini scale hot box for thermal efficiency evaluation of an insulation building block prototype used in Bahrain. *Adv. Build. Energy Res.* **2016**, *11*, 130–151. [[CrossRef](#)]
33. EWA. Thermal Insulation Wall Cross Section—Welcome to Ewa Website. Electricity and Water Authority. Available online: [https://www.ewa.bh/en/Conservation/Electricity/Documents/Thermal%20Insulation\\_Wall\\_Cross%20section\\_2020-06-25.pdf](https://www.ewa.bh/en/Conservation/Electricity/Documents/Thermal%20Insulation_Wall_Cross%20section_2020-06-25.pdf) (accessed on 5 June 2024).
34. Mavromatidis, L.; Michel, P.; El Mankibi, M.; Santamouris, M. Study on transient heat transfer through multilayer thermal insulation: Numerical analysis and experimental investigation. *Build. Simul.* **2010**, *3*, 279–294. [[CrossRef](#)]
35. Mavromatidis, L.; El Mankibi, M.; Michel, P.; Santamouris, M. Numerical estimation of time lags and decrement factors for wall complexes including multilayer thermal insulation in two different climate zones. *Appl. Energy* **2012**, *92*, 480–491. [[CrossRef](#)]
36. Weather and Climate for a Trip to Bahrain: When is the Best Time to Go? Available online: <https://Hikersbay.com/climate/bahrain> (accessed on 5 June 2024).
37. Bahrain, Bahrain Climate Averages, Monthly Weather Conditions. Available online: <https://www.weatherworld.com/yearly-climate/bh/bahrain.html> (accessed on 5 June 2024).
38. Bayram, I.; Al-Qahtani, M.; Saddouri, F.; Koc, M. Estimating the Cost of Summer Cooling in Bahrain. In Proceedings of the IEEE GCC Conference and Exhibition (GCCCE), Manama, Bahrain, 8–11 May 2017; Volume 9. [[CrossRef](#)]
39. Picotech.com/TC-08 Thermocouple Data Logger | Specifications. Available online: <https://www.picotech.com/data-logger/tc-08/thermocouple-data-logger> (accessed on 5 June 2024).
40. Yun, T.S.; Jeong, Y.J.; Youm, K.-S. Effect of surrogate aggregates on the thermal conductivity of concrete at ambient and elevated temperatures. *Sci. World J.* **2014**, *2014*, 939632. [[CrossRef](#)]
41. Amir, A.; Alibaba, H. Comparison between Heat Conductivity of EPS (Expanded Polystyrene) and XPS (Extruded Polystyrene). *Int. J. Recent Res. Civ. Mech. Eng.* **2018**, *4*, 24–31.

**Disclaimer/Publisher’s Note:** The statements, opinions and data contained in all publications are solely those of the individual author(s) and contributor(s) and not of MDPI and/or the editor(s). MDPI and/or the editor(s) disclaim responsibility for any injury to people or property resulting from any ideas, methods, instructions or products referred to in the content.